学位論文(要約)

Multifunctional molecular magnet based on octacyanometalate

(オクタシアノ金属錯体を構築素子とした

多機能性分子磁性体)

平成２５年１２月博士（理学）

申請

東京大学大学院理学系研究科

化学専攻

井元　健太

Index

Chapter 1 Introduction

1.1 Molecule-based magnet[1-8]

Our laboratory has reported a lot of functional magnetic materials and unique magnetic properties using cyano-bridged metal assemblies, which are classified as molecule-based magnets.[1-8] For example, as functional magnetic materials, our laboratory has reported photo-induced magnetization in which a substance is optically switched between paramagnetic state and ferromagnetic state,[9-13] humidity sensitive magnet which exhibit humidity-induced reversible change of magnetic properties and/or magnetic pole direction,[14,15] thermal phase transition phenomenon with large thermal hysteresis,[16-17] etc. In addition, as unique magnetic properties, we have reported mixed ferro-ferri magnetism,[18-19] inverted magnetic hysteresis loop,[20] magnetic dimensional crossover phenomenon,[21] etc. In this section, first of all, I will introduce about molecule-based magnet; what kind of compound is classified as a molecule-based magnet, and what is the characteristic of molecule-based magnets. Molecule-based magnets are magnetic materials composed of metal complex, organic radical, or charge transfer complex based on metal complex and/or organic radical, whose molecular characteristics (electronic spectrum, redox properties, etc.) had been drawn attention.[1-8] Molecule-based magnets can take various colors,[22] which are usually not realized in black or metallic colored metal oxide or magnetic metals. In addition, since molecule-based magnets can change their crystal structure and/or electronic state by various external stimuli, they are extensively studied as functional magnetic materials, in which magnetic properties are changed by various external stimuli, such as solvent, humidity, pressure, or light. The researches about the magnetic properties of metal complexes have been executed in the 1950's before the appearance of the term "molecule-based magnet".[23-32] Most of these researches are devoted to theoretical treatment of magnetic properties of mononuclear metal complex without magnetic interaction, or those of di- or tri-nuclear complexes. Such works about magnetic properties of isolated metal complexes or polynuclear complexes lead to the discovery of slow magnetic relaxation in highly anisotropic materials called as single molecule magnet and the subsequent extensive investigations,[33-36] but I do not introduce further about single molecule magnet because this phenomenon is different from the bulk magnetization on which our laboratory has been focused. The bulk magnetic properties of metal complexes started from late 1980's.[37-39] These researches succeeded in obtaining bulk magnetic materials by using designable advantage of metal complex or organic radicals, e.g., assembling metal ions as designed using coordination bond and/or controlling the electronic states of metal ions or organic radicals by considering redox potential. In addition, metal-free organic radical magnet has been realized[40] and

ferromagnetic materials have been realized in a variety of compounds. In such stream of research, Prussian blue analogs have been reported as a molecule-based magnet in 1986.[41] Afterwards, various functions such as room-temperature magnetism,[42-45] humidity-induced magnetism,[15] photo-induced magnetism[9-13,46-48] have been realized in Prussian blue analogues. Additionally, heptacyanometalate-based magnets[49-52] or octacyanometalate-based magnets[53-59] were proved to be useful as molecule-based magnets and various functionalities have been demonstrated according to the characteristics of the components. From the next section, I will introduce the following background knowledge in the field of molecule-based magnet: molecular-field theory in which thermodynamical treatment is considered to describe magnetic susceptibility and magnetic phase transition, molecular field theory for more than binary metal system developed from our laboratory, Van Vleck paramagnetism, which is often applied to understand magnetic properties of single metal ion and polynuclear metal complexes, background and functionalities in cyano-bridged metal assemblies and their functionalities, and, spin-crossover phenomenon and ionic conductivity, which are focused on in this thesis.

1.2 Molecular field theory

i) Molecular field theory for unary metal system[60]

Molecular field theory is the first theory which succeeded in explaining ferromagnetic phase transition, which is mainly developed by P. Weiss and L. Néel. In this theory, the magnetic interaction is introduced as molecular field, which is proportional to the magnetization value (M) at the neighbor site, the number of neighbor sites (z), and superexchange interaction parameter (J). For unary metal system, when the magnetic moment is M, the molecular field H_M is expressed as

$$H_M = H_0 + nM \text{ , where } n = \frac{2Z}{N_A (g\mu_B)^2} J \text{ .} \quad (1)$$

Here, H_o is the external magnetic field, N_A is Abogadro constant, g is g factor, μ_B is Bohr magneton, and Z is the number of the nearest neighbor metal sites (coordination number of bridging ligand). The averaged sublattice magnetization ($<M>$, where $M = N_A g\mu_B <M>$) is obtained by solving self-consistent equation,

$$< M >= S_M B_{S_M} (\frac{g\mu_B H_M S_M}{k_B T}) \quad (2)$$

,where S_M is spin quantum number of the metal and B_{S_M} is the Brillouin function, which is given by the following formula,

$$B_{S_M}(a) = (\frac{2S_M + 1}{2S_M})\tanh^{-1}(\frac{2S_M + 1}{2S_M} a) - (\frac{1}{2S_M})\tanh^{-1}(\frac{1}{2S_M} a) \text{ .} \quad (3)$$

To obtain spontaneous magnetization, we set $H_0 = 0$ and the equation is expressed as

$$< M >= S_{\mathrm{M}} B_{S_{\mathrm{M}}}(\frac{g\mu_{\mathrm{B}} H_{\mathrm{M}} S_{\mathrm{M}}}{k_{\mathrm{B}} T}) = S_{\mathrm{M}} B_{S_{\mathrm{M}}}(\frac{2ZJS_{\mathrm{M}}}{k_{\mathrm{B}} T} < M >) . \quad (4)$$

When $x = \frac{2ZJS_{\mathrm{M}}}{k_{\mathrm{B}} T} < M >$ is introduced, the equation becomes

$$< M >= \frac{k_{\mathrm{B}} T}{2ZJS_{\mathrm{M}}} x \quad (5)$$

and

$$< M >= S_{\mathrm{M}} B_{S_{\mathrm{M}}}(x) . \quad (6)$$

The solution <*M*> is obtained by the intersection of <*M*> vs *x* curves of equations (5) and (6). As depicted in Figure 1.1, *M* value takes non-zero value below specific temperature T_{C}, where tangent line of $M = S_{\mathrm{M}} B_{S_{\mathrm{M}}}(x)$ at $x = 0$ coincides with $< M >= \frac{k_{\mathrm{B}} T}{2ZJS_{\mathrm{M}}} x$. The T_{C} value corresponds to the Curie temperature and is obtained as

$$T_{\mathrm{C}} = \frac{2ZJS_{\mathrm{M}}(S_{\mathrm{M}} + 1)}{3k_{\mathrm{B}}} . \quad (7)$$

as the following way.

Around T_{C}, *x* value is almost zero. In this region we can apply the approximation of Brillouin function with $x << 1$. When $x << 1$, $B_{S_{\mathrm{M}}}(x)$ is approximated as

$$B_{S_{\mathrm{M}}}(x) \approx \frac{S_{\mathrm{M}} + 1}{3S_{\mathrm{M}}} x . \quad (8)$$

Therefore, the θ value is obtained as

$$\begin{aligned} & S_{\mathrm{M}} \frac{S_{\mathrm{M}} + 1}{3S_{\mathrm{M}}} x = \frac{k_{\mathrm{B}} T_{\mathrm{C}}}{2ZJS_{\mathrm{M}}} x \\ \Leftrightarrow & \frac{S_{\mathrm{M}} + 1}{3} = \frac{k_{\mathrm{B}} T_{\mathrm{C}}}{2ZJS_{\mathrm{M}}} \\ \Leftrightarrow & T_{\mathrm{C}} = \frac{2ZJS_{\mathrm{M}}(S_{\mathrm{M}} + 1)}{3k_{\mathrm{B}}} \end{aligned} \quad (9)$$

Equation (9) enables us to estimate superexchange interaction parameter (*J*) by Curie temperature (T_{C}).

From here, we consider the magnetic susceptibility (χ) at high temperature region. In this case, we include external magnetic field (H_0) in equation (4) and the equation is

$$< M >= S_{\mathrm{M}} B_{S_{\mathrm{M}}}\{\frac{g\mu_{\mathrm{B}} S_{\mathrm{M}}}{k_{\mathrm{B}} T}(H_0 + \frac{2ZJ}{g\mu_{\mathrm{B}}} < M >)\} . \quad (10)$$

At high temperature, $\frac{g\mu_{\mathrm{B}} S_{\mathrm{M}}}{k_{\mathrm{B}} T}(H_0 + \frac{2ZJ}{g\mu_{\mathrm{B}}} < M >) << 1$, therefore,

$$< M >= \frac{S_M + 1}{3} \frac{g\mu_B S_M}{k_B T} (H_0 + \frac{2ZJ}{g\mu_B} < M >) . \quad (11)$$

Introducing $\chi = M/H_0 = N_A g\mu_B < M > /H_0$,

$$\chi = \frac{S_M + 1}{3} \frac{N_A (g\mu_B)^2 S_M}{k_B T} (1 + \frac{2ZJ}{N_A (g\mu_B)^2} \chi)$$

$$\Leftrightarrow \quad (T - \frac{2ZJS_M(S_M + 1)}{3k_B}) \chi = \frac{N_A (g\mu_B)^2 S_M (S_M + 1)}{3k_B}$$

$$\Leftrightarrow \chi = \frac{C}{T - \theta} \quad .$$

$$\Leftrightarrow \frac{1}{\chi} = \frac{T - \theta}{C} \quad (12)$$

This magnetic behavior is called Curie-Weiss law and $C = \frac{N_A (g\mu_B)^2 S_M (S_M + 1)}{3k_B}$ is called Curie constant. θ is Weiss temperature, which is positive for ferromagnetic interaction ($J > 0$) and is negative for antiferromagnetic interaction ($J < 0$). In addition, Curie temperature (T_C) is related with θ by $T_C = |\theta|$ in this theory.

The magnetic interaction is clearly understood by plotting χ^{-1} vs T (Figure 1.2).

ii) Molecular field theory for more than binary metal system[18-19]

Detail discussion about magnetic properties of cyano-bridge metal assemblies was performed by Ohkoshi et al. in 1997. They focused on the magnetic interaction only between the nearest neighbor metal sites which is the feature of cyano-bridged metal assemblies and applied molecular field theory to ternary metal Prussian blue analogs. When we consider the formula of $(M_{A\,x} M_{B\,1-x})_{y1}[M_C(CN)_6]_{y2} \cdot zH_2O$ composed of three metal ions of M_A, M_B, and M_C, the molecular field H_M are expressed by the following equation using molecular field coefficient (n_{pq}),

$$H_A = H_0 + n_{AC} M_C , \quad H_B = H_0 + n_{BC} M_C , H_C = H_0 + n_{CA} M_A + n_{CB} M_B , \quad (13)$$

because the nearest neighboring metal of M_A and M_B are always M_C, and that of M_C is M_A or M_B.

The molecular field coefficients (n_{pq}) are given by the following equation

$$n_{\mathrm{AC}} = \frac{2Z_{\mathrm{AC}}}{y_2 N_{\mathrm{A}} (g\mu_{\mathrm{B}})^2} J_{\mathrm{AC}}, n_{\mathrm{BC}} = \frac{2Z_{\mathrm{BC}}}{y_2 N_{\mathrm{A}} (g\mu_{\mathrm{B}})^2} J_{\mathrm{BC}},$$
$$n_{\mathrm{CA}} = \frac{2Z_{\mathrm{CA}}}{y_1 N_{\mathrm{A}} (g\mu_{\mathrm{B}})^2} J_{\mathrm{AC}}, n_{\mathrm{CB}} = \frac{2Z_{\mathrm{CB}}}{y_1 N_{\mathrm{A}} (g\mu_{\mathrm{B}})^2} J_{\mathrm{CB}}, \quad (14)$$

Here, Z_{pq} is the number of the nearest neighbor metal q sites around a p site (coordination number of bridging ligand to metal ion q around a metal ion p). The averaged sublattice magnetization (<M>, where $M_{\mathrm{A}} = y_1 x N_{\mathrm{A}} g\mu_B <M_{\mathrm{A}}>$, $M_{\mathrm{B}} = y_1(1-x) N_{\mathrm{A}} g\mu_B <M_{\mathrm{B}}>$, $M_{\mathrm{C}} = y_2 N_{\mathrm{A}} g\mu_B <M_{\mathrm{C}}>$) is obtained by the following equations,

$$< M_{\mathrm{A}} >= S_{\mathrm{A}} B_{S_{\mathrm{A}}} (\frac{g\mu_{\mathrm{B}} H_{\mathrm{A}} S_{\mathrm{A}}}{k_{\mathrm{B}} T}),$$
$$< M_{\mathrm{B}} >= S_{\mathrm{B}} B_{S_{\mathrm{B}}} (\frac{g\mu_{\mathrm{B}} H_{\mathrm{B}} S_{\mathrm{B}}}{k_{\mathrm{B}} T}), \quad (15)$$
$$< M_{\mathrm{C}} >= S_{\mathrm{C}} B_{S_{\mathrm{C}}} (\frac{g\mu_{\mathrm{B}} H_{\mathrm{C}} S_{\mathrm{C}}}{k_{\mathrm{B}} T}),$$

.

where S_{M} is spin quantum number of the metal and $B_{S_{\mathrm{M}}}$ is the Brillouin function.

To obtain spontaneous magnetization, we set $H_0 = 0$ and the equation is expressed as

$$< M_{\mathrm{A}} >= S_{\mathrm{A}} B_{S_{\mathrm{A}}} (\frac{g\mu_{\mathrm{B}} n_{\mathrm{AC}} M_{\mathrm{C}} S_{\mathrm{A}}}{k_{\mathrm{B}} T}) = S_{\mathrm{A}} B_{S_{\mathrm{A}}} (\frac{2Z_{\mathrm{AC}} x J_{\mathrm{AC}} S_{\mathrm{A}}}{k_{\mathrm{B}} T} < M_{\mathrm{C}} >), \quad (16\text{-}1)$$

$$< M_{\mathrm{A}} >= S_{\mathrm{A}} B_{S_{\mathrm{A}}} (\frac{g\mu_{\mathrm{B}} n_{\mathrm{AC}} M_{\mathrm{C}} S_{\mathrm{A}}}{k_{\mathrm{B}} T}) = S_{\mathrm{A}} B_{S_{\mathrm{A}}} (\frac{2Z_{\mathrm{AC}} x J_{\mathrm{AC}} S_{\mathrm{A}}}{k_{\mathrm{B}} T} < M_{\mathrm{C}} >), \quad (16\text{-}2)$$

$$< M_{\mathrm{C}} >= S_{\mathrm{C}} B_{S_{\mathrm{C}}} (\frac{g\mu_{\mathrm{B}} (n_{\mathrm{CA}} M_{\mathrm{A}} + n_{\mathrm{CB}} M_{\mathrm{B}}) S_{\mathrm{C}}}{k_{\mathrm{B}} T})$$
$$= S_{\mathrm{C}} B_{S_{\mathrm{C}}} (\frac{2Z_{\mathrm{CA}} x J_{\mathrm{AC}} S_{\mathrm{C}}}{k_{\mathrm{B}} T} < M_{\mathrm{A}} > + \frac{2Z_{\mathrm{CB}} (1-x) J_{\mathrm{BC}} S_{\mathrm{C}}}{k_{\mathrm{B}} T} < M_{\mathrm{B}} >) \quad (16\text{-}3)$$

By solving these self-consistent equations, we can obtain magnetization values of each metal ion and total magnetization value.

The T_{C} value is obtained by the approximating the Brillouin function as $B_{S_{\mathrm{M}}}(x) \approx \frac{S_{\mathrm{M}}+1}{3S_{\mathrm{M}}} x$, which is valid for $x << 1$. In this case, the equations are

$$< M_{\mathrm{A}} >= S_{\mathrm{A}} \frac{S_{\mathrm{A}}+1}{3S_{\mathrm{A}}} \frac{2Z_{\mathrm{AC}} x J_{\mathrm{AC}} S_{\mathrm{A}}}{k_{\mathrm{B}} T_{\mathrm{C}}} < M_{\mathrm{C}} >, \tag{17-1}$$

$$< M_{\mathrm{B}} >= S_{\mathrm{B}} \frac{S_{\mathrm{B}}+1}{3S_{\mathrm{B}}} \frac{2Z_{\mathrm{BC}} (1-x) J_{\mathrm{BC}} S_{\mathrm{B}}}{k_{\mathrm{B}} T_{\mathrm{C}}} < M_{\mathrm{C}} >, \tag{17-2}$$

$$< M_{\mathrm{C}} >= S_{\mathrm{C}} \frac{S_{\mathrm{C}}+1}{3S_{\mathrm{C}}} (\frac{2Z_{\mathrm{CA}} x J_{\mathrm{AC}} S_{\mathrm{C}}}{k_{\mathrm{B}} T_{\mathrm{C}}} < M_{\mathrm{A}} > + \frac{2Z_{\mathrm{CB}} (1-x) J_{\mathrm{BC}} S_{\mathrm{C}}}{k_{\mathrm{B}} T_{\mathrm{C}}} < M_{\mathrm{B}} >), \tag{17-3}$$

therefore,

$$< M_{\mathrm{C}} >= \frac{S_{\mathrm{C}}+1}{3} (\frac{2Z_{\mathrm{CA}} x J_{\mathrm{AC}} S_{\mathrm{C}}}{k_{\mathrm{B}} T} \frac{S_{\mathrm{A}}+1}{3} \frac{2Z_{\mathrm{AC}} x J_{\mathrm{AC}} S_{\mathrm{A}}}{k_{\mathrm{B}} T_{\mathrm{C}}} < M_{\mathrm{C}} >$$

$$+ \frac{2Z_{\mathrm{CB}} (1-x) J_{\mathrm{BC}} S_{\mathrm{C}}}{k_{\mathrm{B}} T_{\mathrm{C}}} \frac{S_{\mathrm{B}}+1}{3} \frac{2Z_{\mathrm{BC}} (1-x) J_{\mathrm{BC}} S_{\mathrm{B}}}{k_{\mathrm{B}} T_{\mathrm{C}}} < M_{\mathrm{C}} >)$$

$$\Leftrightarrow \frac{S_{\mathrm{C}}+1}{3} (\frac{4Z_{\mathrm{CA}} Z_{\mathrm{AC}} x^2 {J_{\mathrm{AC}}}^2 S_{\mathrm{C}}}{3{k_{\mathrm{B}}}^2 {T_{\mathrm{C}}}^2} S_{\mathrm{A}} (S_{\mathrm{A}}+1) + \frac{4Z_{\mathrm{CB}} Z_{\mathrm{BC}} (1-x)^2 {J_{\mathrm{BC}}}^2 S_{\mathrm{C}}}{3{k_{\mathrm{B}}}^2 {T_{\mathrm{C}}}^2} S_{\mathrm{B}} (S_{\mathrm{B}}+1)) = 1$$

$$\Leftrightarrow {T_{\mathrm{C}}}^2 = \frac{4S_{\mathrm{C}} (S_{\mathrm{C}}+1)}{(3k_{\mathrm{B}})^2} (Z_{\mathrm{CA}} Z_{\mathrm{AC}} x^2 {J_{\mathrm{AC}}}^2 S_{\mathrm{A}} (S_{\mathrm{A}}+1) + Z_{\mathrm{CB}} Z_{\mathrm{BC}} (1-x)^2 {J_{\mathrm{BC}}}^2 S_{\mathrm{B}} (S_{\mathrm{B}}+1))$$

$$\Leftrightarrow T_{\mathrm{C}} = \frac{2}{3k_{\mathrm{B}}} \sqrt{S_{\mathrm{C}} (S_{\mathrm{C}}+1) \{Z_{\mathrm{CA}} Z_{\mathrm{AC}} x^2 {J_{\mathrm{AC}}}^2 S_{\mathrm{A}} (S_{\mathrm{A}}+1) + Z_{\mathrm{CB}} Z_{\mathrm{BC}} (1-x)^2 {J_{\mathrm{BC}}}^2 S_{\mathrm{B}} (S_{\mathrm{B}}+1)\}} \tag{18}$$

This equation relates the superexchange interaction parameters (J) and Curie temperature (T_{C}).

As performed in the unary metal system, we consider the magnetic susceptibility (χ) at high temperature region. In this case, we include external magnetic field (H_0) and the equation is

$$< M_{\mathrm{A}} >= S_{\mathrm{A}} B_{S_{\mathrm{A}}} (\frac{g\mu_{\mathrm{B}} H_{\mathrm{A}} S_{\mathrm{A}}}{k_{\mathrm{B}} T}) = S_{\mathrm{A}} B_{S_{\mathrm{A}}} (\frac{g\mu_{\mathrm{B}} (H_0 + n_{\mathrm{AC}} M_{\mathrm{C}}) S_{\mathrm{A}}}{k_{\mathrm{B}} T}), \tag{19-1}$$

$$< M_{\mathrm{B}} >= S_{\mathrm{B}} B_{S_{\mathrm{B}}} (\frac{g\mu_{\mathrm{B}} H_{\mathrm{B}} S_{\mathrm{B}}}{k_{\mathrm{B}} T}) = S_{\mathrm{B}} B_{S_{\mathrm{B}}} (\frac{g\mu_{\mathrm{B}} (H_0 + n_{\mathrm{BC}} M_{\mathrm{C}}) S_{\mathrm{B}}}{k_{\mathrm{B}} T}), \tag{19-2}$$

$$< M_{\mathrm{C}} >= S_{\mathrm{C}} B_{S_{\mathrm{C}}} (\frac{g\mu_{\mathrm{B}} H_{\mathrm{C}} S_{\mathrm{C}}}{k_{\mathrm{B}} T}) = S_{\mathrm{C}} B_{S_{\mathrm{C}}} (\frac{g\mu_{\mathrm{B}} (H_0 + n_{\mathrm{CA}} M_{\mathrm{A}} + n_{\mathrm{CB}} M_{\mathrm{B}}) S_{\mathrm{B}}}{k_{\mathrm{B}} T}). \tag{19-3}$$

Because we consider the magnetization at high temperature, we introduce the approximation of the Brillouin function as $B_{S_{\mathrm{M}}}(x) \approx \frac{S_{\mathrm{M}}+1}{3S_{\mathrm{M}}} x$ again. Then the equation is

$$\frac{M_{\mathrm{A}}}{y_1 x N_{\mathrm{A}} g\mu_{\mathrm{B}}} = \frac{S_{\mathrm{A}}+1}{3}\left(\frac{g\mu_{\mathrm{B}}(H_0 + n_{\mathrm{AC}}M_{\mathrm{C}})S_{\mathrm{A}}}{k_{\mathrm{B}}T}\right), \tag{20-1}$$

$$\frac{M_{\mathrm{B}}}{y_1 (1-x) N_{\mathrm{A}} g\mu_{\mathrm{B}}} = \frac{S_{\mathrm{B}}+1}{3}\left(\frac{g\mu_{\mathrm{B}}(H_0 + n_{\mathrm{BC}}M_{\mathrm{C}})S_{\mathrm{B}}}{k_{\mathrm{B}}T}\right), \tag{20-2}$$

$$\frac{M_{\mathrm{C}}}{y_2 N_{\mathrm{A}} g\mu_{\mathrm{B}}} = \frac{S_{\mathrm{C}}+1}{3}\left(\frac{g\mu_{\mathrm{B}}(H_0 + n_{\mathrm{CA}}M_{\mathrm{A}} + n_{\mathrm{CB}}M_{\mathrm{B}})S_{\mathrm{C}}}{k_{\mathrm{B}}T}\right). \tag{20-3}$$

Introducing $\chi_i = M_i / H_0$,

$$\chi_{\mathrm{A}} = y_1 x \frac{N_{\mathrm{A}}(g\mu_{\mathrm{B}})^2 S_{\mathrm{A}}(S_{\mathrm{A}}+1)}{3k_{\mathrm{B}}T}(1 + n_{\mathrm{AC}}\chi_{\mathrm{C}}), \tag{21-1}$$

$$\chi_{\mathrm{B}} = y_1 (1-x) \frac{N_{\mathrm{A}}(g\mu_{\mathrm{B}})^2 S_{\mathrm{B}}(S_{\mathrm{B}}+1)}{3k_{\mathrm{B}}T}(1 + n_{\mathrm{BC}}\chi_{\mathrm{C}}), \tag{21-2}$$

$$\chi_{\mathrm{C}} = y_2 \frac{N_{\mathrm{A}}(g\mu_{\mathrm{B}})^2 S_{\mathrm{C}}(S_{\mathrm{C}}+1)}{3k_{\mathrm{B}}T}(1 + n_{\mathrm{CA}}\chi_{\mathrm{A}} + n_{\mathrm{CB}}\chi_{\mathrm{B}}). \tag{21-3}$$

Using Curie constants (C_i), $C_i = \frac{N_{\mathrm{A}}(g\mu_{\mathrm{B}})^2 S_i(S_i+1)}{3k_{\mathrm{B}}}$,

$$\chi_{\mathrm{A}} = y_1 x \frac{C_{\mathrm{A}}}{T}(1 + n_{\mathrm{AC}}\chi_{\mathrm{C}}), \tag{22-1}$$

$$\chi_{\mathrm{B}} = y_1 (1-x) \frac{C_{\mathrm{B}}}{T}(1 + n_{\mathrm{BC}}\chi_{\mathrm{C}}), \tag{22-2}$$

$$\chi_{\mathrm{C}} = y_2 \frac{C_{\mathrm{C}}}{T}(1 + n_{\mathrm{CA}}\chi_{\mathrm{A}} + n_{\mathrm{CB}}\chi_{\mathrm{B}}). \tag{22-3}$$

From these equations, χ_{C}, χ_{A}, χ_{B} , and $\chi = \chi_{\mathrm{A}} + \chi_{\mathrm{B}} + \chi_{\mathrm{C}}$ are obtained as

$$\chi_{\mathrm{C}} = y_2 \frac{C_{\mathrm{C}}}{T}\{1 + n_{\mathrm{CA}} y_1 x \frac{C_{\mathrm{A}}}{T}(1 + n_{\mathrm{AC}}\chi_{\mathrm{C}}) + n_{\mathrm{CB}} y_1 (1-x)\frac{C_{\mathrm{B}}}{T}(1 + n_{\mathrm{BC}}\chi_{\mathrm{C}})\}$$

$$\Leftrightarrow \chi_{\mathrm{C}}(1 - n_{\mathrm{CA}} n_{\mathrm{AC}} y_1 x \frac{C_{\mathrm{A}}}{T} - n_{\mathrm{CB}} n_{\mathrm{BC}} y_1 (1-x)\frac{C_{\mathrm{B}}}{T})$$

$$= y_2 \frac{C_{\mathrm{C}}}{T}\{1 + n_{\mathrm{CA}} y_1 x \frac{C_{\mathrm{A}}}{T} + n_{\mathrm{CB}} y_1 (1-x)\frac{C_{\mathrm{B}}}{T}\}$$

$$\therefore \quad \chi_{\mathrm{C}} = \frac{y_2 C_{\mathrm{C}}\{T + n_{\mathrm{CA}} y_1 x C_{\mathrm{A}} + n_{\mathrm{CB}} y_1 (1-x) C_{\mathrm{B}}\}}{T^2 - \{n_{\mathrm{CA}} n_{\mathrm{AC}} y_1 x C_{\mathrm{A}} + n_{\mathrm{CB}} n_{\mathrm{BC}} y_1 (1-x) C_{\mathrm{B}}\}T}$$

$$= y_2 \frac{C_{\mathrm{C}}}{T}\frac{\{T^2 + n_{\mathrm{CA}} y_1 x C_{\mathrm{A}} T + n_{\mathrm{CB}} y_1 (1-x) C_{\mathrm{B}} T\}}{T^2 - \{n_{\mathrm{CA}} n_{\mathrm{AC}} y_1 x C_{\mathrm{A}} + n_{\mathrm{CB}} n_{\mathrm{BC}} y_1 (1-x) C_{\mathrm{B}}\}T}$$

$$= y_2 \frac{C_{\mathrm{C}}}{T}[1 + \frac{(1 + n_{\mathrm{AC}}) n_{\mathrm{CA}} y_1 x C_{\mathrm{A}} T + (1 + n_{\mathrm{BC}}) n_{\mathrm{CB}} y_1 (1-x) C_{\mathrm{B}} T}{T^2 - \{n_{\mathrm{CA}} n_{\mathrm{AC}} y_1 x C_{\mathrm{A}} + n_{\mathrm{CB}} n_{\mathrm{BC}} y_1 (1-x) C_{\mathrm{B}}\}T}, \tag{23-1}$$

$$\chi_{\mathrm{A}} = y_1 x \frac{C_{\mathrm{A}}}{T}[1 + n_{\mathrm{AC}} \frac{y_2 C_{\mathrm{C}}\{T + n_{\mathrm{CA}} y_1 x C_{\mathrm{A}} + n_{\mathrm{CB}} y_1 (1-x) C_{\mathrm{B}}\}}{T^2 - \{n_{\mathrm{CA}} n_{\mathrm{AC}} y_1 x C_{\mathrm{A}} + n_{\mathrm{CB}} n_{\mathrm{BC}} y_1 (1-x) C_{\mathrm{B}}\}T}]$$

$$= y_1 x \frac{C_{\mathrm{A}}}{T}[1 + \frac{n_{\mathrm{AC}} y_2 C_{\mathrm{C}} T + n_{\mathrm{AC}} y_2 C_{\mathrm{C}} n_{\mathrm{CA}} y_1 x C_{\mathrm{A}} + n_{\mathrm{AC}} y_2 C_{\mathrm{C}} n_{\mathrm{CB}} y_1 (1-x) C_{\mathrm{B}}}{T^2 - \{n_{\mathrm{CA}} n_{\mathrm{AC}} y_1 x C_{\mathrm{A}} + n_{\mathrm{CB}} n_{\mathrm{BC}} y_1 (1-x) C_{\mathrm{B}}\}T}], \tag{23-2}$$

$$\chi_{\mathrm{B}} = y_1 (1-x) \frac{C_{\mathrm{B}}}{T}[1 + n_{\mathrm{BC}} \frac{y_2 C_{\mathrm{C}}\{T + n_{\mathrm{CA}} y_1 x C_{\mathrm{A}} + n_{\mathrm{CB}} y_1 (1-x) C_{\mathrm{B}}\}}{T^2 - \{n_{\mathrm{CA}} n_{\mathrm{AC}} y_1 x C_{\mathrm{A}} + n_{\mathrm{CB}} n_{\mathrm{BC}} y_1 (1-x) C_{\mathrm{B}}\}T}]$$

$$= y_1 (1-x) \frac{C_{\mathrm{B}}}{T}[1 + \frac{n_{\mathrm{BC}} y_2 C_{\mathrm{C}} T + n_{\mathrm{BC}} y_2 C_{\mathrm{C}} n_{\mathrm{CA}} y_1 x C_{\mathrm{A}} + n_{\mathrm{BC}} y_2 C_{\mathrm{C}} n_{\mathrm{CB}} y_1 (1-x) C_{\mathrm{B}}\}}{T^2 - \{n_{\mathrm{CA}} n_{\mathrm{AC}} y_1 x C_{\mathrm{A}} + n_{\mathrm{CB}} n_{\mathrm{BC}} y_1 (1-x) C_{\mathrm{B}}\}T}], \tag{23-3}$$

and

$$\begin{aligned}\chi = {} & y_1 x \frac{C_{\mathrm{A}}}{T}[1 + \frac{n_{\mathrm{AC}} y_2 C_{\mathrm{C}} T + n_{\mathrm{AC}} y_2 C_{\mathrm{C}} n_{\mathrm{CA}} y_1 x C_{\mathrm{A}} + n_{\mathrm{AC}} y_2 C_{\mathrm{C}} n_{\mathrm{CB}} y_1 (1-x) C_{\mathrm{B}}}{T^2 - \{n_{\mathrm{CA}} n_{\mathrm{AC}} y_1 x C_{\mathrm{A}} + n_{\mathrm{CB}} n_{\mathrm{BC}} y_1 (1-x) C_{\mathrm{B}}\}T} \\ & + y_1 (1-x) \frac{C_{\mathrm{B}}}{T}[1 + \frac{n_{\mathrm{BC}} y_2 C_{\mathrm{C}} T + n_{\mathrm{BC}} y_2 C_{\mathrm{C}} n_{\mathrm{CA}} y_1 x C_{\mathrm{A}} + n_{\mathrm{BC}} y_2 C_{\mathrm{C}} n_{\mathrm{CB}} y_1 (1-x) C_{\mathrm{B}}\}}{T^2 - \{n_{\mathrm{CA}} n_{\mathrm{AC}} y_1 x C_{\mathrm{A}} + n_{\mathrm{CB}} n_{\mathrm{BC}} y_1 (1-x) C_{\mathrm{B}}\}T} \\ & + y_2 \frac{C_{\mathrm{C}}}{T}[1 + \frac{(1 + n_{\mathrm{AC}}) n_{\mathrm{CA}} y_1 x C_{\mathrm{A}} T + (1 + n_{\mathrm{BC}}) n_{\mathrm{CB}} y_1 (1-x) C_{\mathrm{B}} T}{T^2 - \{n_{\mathrm{CA}} n_{\mathrm{AC}} y_1 x C_{\mathrm{A}} + n_{\mathrm{CB}} n_{\mathrm{BC}} y_1 (1-x) C_{\mathrm{B}}\}T}\end{aligned} \tag{24}$$

where

$$\begin{aligned} & n_{\mathrm{AC}} = \frac{2Z_{\mathrm{AC}}}{y_2 N_{\mathrm{A}} (g\mu_{\mathrm{B}})^2} J_{\mathrm{AC}}, n_{\mathrm{BC}} = \frac{2Z_{\mathrm{BC}}}{y_2 N_{\mathrm{A}} (g\mu_{\mathrm{B}})^2} J_{\mathrm{BC}}, \\ & n_{\mathrm{CA}} = \frac{2Z_{\mathrm{CA}}}{y_1 N_{\mathrm{A}} (g\mu_{\mathrm{B}})^2} J_{\mathrm{AC}}, n_{\mathrm{CB}} = \frac{2Z_{\mathrm{CB}}}{y_1 N_{\mathrm{A}} (g\mu_{\mathrm{B}})^2} J_{\mathrm{CB}}. \end{aligned} \tag{25}$$

The lease square fitting of the experimental magnetic susceptibility allows us to estimate the superexchange interaction constant (J) and g factor.

1.3 Van Vleck paramagnetism[23]

i) Van Vleck equation

Van Vleck theory is developed to perform theoretical treatment of magnetic properties of mononuclear or polynuclear metal complexes. This theory is based on quantum chemical approach and we calculate magnetic susceptibility by taking account of Boltzmann distribution of each energy state which is split by Zeeman effect, spin-orbit coupling, and exchange interaction (spin-spin coupling). The Van Vleck equation is obtained by considering Zeeman effect as follows.

The magnetization value (I) is related to the energy value of a material (W) as

$$I = -\frac{\partial W}{\partial H}, \tag{26}$$

where H is the external magnetic field.

When we consider that an atom is placed in an external magnetic field, the energy of level i (W_i) can be expanded as

$$W_i = W_i^{(0)} + W_i^{(1)}H + W_i^{(2)}H^2 + o(H^3), \tag{27}$$

where $W_i^{(1)}$, $W_i^{(2)}$, … are called as first, second, … order Zeeman coefficients.

Ignoring the third and higher order term,

$$I_i = -\frac{\partial W}{\partial H} = -W_i^{(1)} - 2W_i^{(2)}H . \tag{28}$$

Considering the Boltzmann distribution of each state, the magnetic susceptibility ($\chi = I / H$) is

$$\chi = \frac{N}{H}\frac{\sum I_i \exp(W_i/kT)}{\sum \exp(W_i/kT)} = \frac{(N/H)\sum(-W_i^{(1)} - 2W_i^{(2)}H)\exp(W_i/kT)}{\sum \exp(W_i/kT)}, \tag{29}$$

where N is Avogadro constant. Considering the order of Zeeman energy is a few wavenumber and $k \sim 0.695$ cm^{-1}, at high temperature region, the approximation of $W_i^{(1)} << kT$ can be applied. In this condition,

$\exp(W_i^{(1)}/kT) \sim 1 - W_i^{(1)}/kT$ and $\exp(W_i^{(2)}/kT) \sim 1 - W_i^{(2)}/kT$, so

$$\exp(-W_i/kT) = \exp(-W_i^{(0)} - W_i^{(1)}H - W_i^{(2)}H^2)$$
$$= \exp(-W_i^{(0)})(1 - W_i^{(1)}H/kT)(1 - W_i^{(2)}H^2/kT)$$
$$\sim \exp(-W_i^{(0)})(1 - W_i^{(1)}H/kT)$$

Therefore,

$$\begin{aligned}\chi &= \frac{(N/H)\sum(-W_i^{(1)} - 2W_i^{(2)}H)\exp(W_i/kT)}{\sum\exp(W_i/kT)} \\ &= \frac{(N/H)\sum(-W_i^{(1)} - 2W_i^{(2)}H)\exp(-W_i^{(0)}/kT)(1-W_i^{(1)}H/kT)}{\sum\exp(-W_i^{(0)}/kT)(1-W_i^{(1)}H/kT)} \\ &= \frac{N\sum(-W_i^{(1)}/H)\exp(-W_i^{(0)}/kT) + N\sum\{(W_i^{(1)})^2 - 2W_i^{(2)}\}\exp(-W_i^{(0)}/kT)}{\sum\exp(-W_i^{(0)}/kT)(1-W_i^{(1)}H/kT)} \\ &+ \frac{N\sum(2W_i^{(1)}W_i^{(2)}H/kT)\exp(-W_i^{(0)}/kT)}{\sum\exp(-W_i^{(0)}/kT)(1-W_i^{(1)}H/kT)}.\end{aligned} \tag{30}$$

Here, noting that Zeeman splitting does not change the average energy value, all terms which have odd order of $W_i^{(1)}$ become zero. Therefore,

$$\begin{aligned}\chi &= \frac{N\sum(-W_i^{(1)}/H)\exp(-W_i^{(0)}/kT) + N\sum\{(W_i^{(1)})^2 - 2W_i^{(2)}\}\exp(-W_i^{(0)}/kT)}{\sum\exp(-W_i^{(0)}/kT)(1-W_i^{(1)}H/kT)} \\ &+ \frac{N\sum(2W_i^{(1)}W_i^{(2)}H/kT)\exp(-W_i^{(0)}/kT)}{\sum\exp(-W_i^{(0)}/kT)(1-W_i^{(1)}H/kT)} \\ &= \frac{N\sum\{(W_i^{(1)})^2 - 2W_i^{(2)}\}\exp(-W_i^{(0)}/kT)}{\sum\exp(-W_i^{(0)}/kT)}.\end{aligned} \tag{31}$$

When we calculate magnetic susceptibility, we obtain $W_i^{(1)}$, $W_i^{(2)}$ by considering spin-orbit coupling, and exchange interaction (spin-spin coupling), and Zeeman splitting, and then we assign the obtained values to the above equations. When Zeeman splitting is smaller enough than spin-orbit coupling and/or exchange interaction, we can treat Zeeman splitting as perturbation. The example calculation of magnetic susceptibility of octahedral Fe(II) ion (d^6) is given in the following.

ii) Magnetic susceptibility of octahedral Fe(II) ion (d^6) with $^5T_2$ term[28]

As an example, I will introduce the calculation of magnetic susceptibility of octahedral Fe(II) ion is given in the following.

When we consider free ion, the five d orbitals are degenerated and the orbital magnetic quantum number (M_L) is a good quantum number. Here, we represent d orbitals by $|M_L\rangle$ (M_L = 2,1,0,-1,-2), which is a eigenstate corresponding to the eigenvalue of M_L. However, in octahedral field, the energy of d orbital splits into three t_{2g} orbitals and two e_g orbitals and the orbital magnetic quantum number (M_L) is no longer a good quantum number. Taking the

principle axis with 4-fold rotation axis, the ground states of octahedral Fe(II) ion (d^6) are triply degenerated and are expressed by the linear combination of $|M_L\rangle$ as

$$|1\rangle, |-1\rangle, \text{and} \sqrt{\frac{1}{2}}\left(|2\rangle - |-2\rangle\right).$$

Considering that the Fe(II) ion (d^6) has spin quantum number (S) of 2, the wavefunctions of $^5T_2$ term is described as the following 15 wavefunctions shown as $|m_L\rangle[m_S]$.

$$\begin{array}{l}
|1\rangle[+2], \quad |1\rangle[+1], \quad |1\rangle[0], \quad |1\rangle[-1], \quad |1\rangle[-2], \\
-|1\rangle[+2], \quad |-1\rangle[+1], \quad |-1\rangle[0], \quad |-1\rangle[-1], \quad |-1\rangle[-2] \\
\sqrt{1/2}(|+2\rangle - |-2\rangle)[+2], \sqrt{1/2}(|+2\rangle - |-2\rangle)[+1], \\
\sqrt{1/2}(|+2\rangle - |-2\rangle)[0], \sqrt{1/2}(|+2\rangle - |-2\rangle)[-1], \sqrt{1/2}(|+2\rangle - |-2\rangle)[-2]
\end{array}$$

From here, we are going to consider the spin-orbit coupling (λ) as the following Hamiltonian.

$H = \lambda LS$.

The interaction among the above 15 wavefunctions can be obtained by the following relation,

$$\begin{array}{l}
\boldsymbol{L_z}|L,M_L,S,M_S\rangle = M_L|L,M_L,S,M_S\rangle \\
\boldsymbol{L_+}|L,M_L,S,M_S\rangle = \sqrt{L(L+1)-M_L(M_L+1)}|L,M_L+1,S,M_S\rangle \\
\boldsymbol{L_-}|L,M_L,S,M_S\rangle = \sqrt{L(L+1)-M_L(M_L-1)}|L,M_L-1,S,M_S\rangle \\
\boldsymbol{S_z}|L,M_L,S,M_S\rangle = M_S|L,M_L,S,M_S\rangle \\
\boldsymbol{S_+}|L,M_L,S,M_S\rangle = \sqrt{S(S+1)-M_S(M_S+1)}|L,M_L,S+1,M_S\rangle \\
\boldsymbol{S_-}|L,M_L,S,M_S\rangle = \sqrt{S(S+1)-M_S(M_S-1)}|L,M_L,S-1,M_S\rangle
\end{array} \tag{32}$$

where L, M_L, S, and M_S is are azimuthal quantum number, orbital magnetic quantum number, spin quantum number, and the z-projection of spin quantum number. As a result, we can obtain the 15 × 15 matrix based on $\left\langle L_i,M_{L_i},S_i,M_{S_i}\left|\lambda LS\right|L_j,M_{L_j},S_j,M_{S_j}\right\rangle$ as shown in Figure 1.3.

By block diagonalization of this 15 × 15 matrix, we have only to solve three 3 × 3 matrices and two 2 × 2 matrices, and other two eigenvalues are diagonal elements without non-diagonal components. By diagonalization, we obtain the eigenenergies ($W^{(0)}$) as shown below,

$W^{(0)} = 3\lambda$ ($g = 3$), $W^{(0)} = \lambda$ ($g = 5$), $W^{(0)} = -2\lambda$ ($g = 7$),

where g is the degree of degeneracy.

Next, we consider Zeeman splitting of these eigenfunctions.

The Zeeman energy is obtained by the following equation,

$$\text{1st order Zeeman energy:}\quad E_{iz}^{(1)} = \mu_B \sum_j \left\langle \psi_i^{(0)} \middle| L_z + 2S_z \middle| \psi_j^{(0)} \right\rangle \tag{33}$$

$$\text{2nd order Zeeman energy:}\quad E_{iz}^{(2)} = \mu_B^2 \sum_j \frac{\left\langle \psi_i^{(0)} \middle| L_z + 2S_z \middle| \psi_j^{(0)} \right\rangle \left\langle \psi_i^{(0)} \middle| L_z + 2S_z \middle| \psi_j^{(0)} \right\rangle}{E_i^{(0)} - E_j^{(0)}} \tag{34}$$

Here, we have only to consider *z* component because *x*, *y*, and *z* are isotropic in this calculation. 1st order Zeeman splitting occurs only between the degenerated eigenfunctions, whereas 2nd order Zeeman splitting should be considered between the eigenfunctions with different energies. As a result, we obtain first and second order Zeeman energy ($W^{(1)}$ and $W^{(2)}$) as described in Figure 1.4.

By substituting the obtained energy values to the Van Vleck equation, we can obtain the following magnetic susceptibility.

$$\chi = \frac{3[28x + \frac{28}{3} + (\frac{45}{2}x + \frac{25}{6})\exp(-3x) + (\frac{49}{2}x - \frac{27}{2})\exp(-5x)]}{8Tx[7 + 5\exp(-3x) + 3\exp(-5x)]}, \tag{35}$$

where $x = kT / \lambda$.

The spin-orbit coupling constant of free Fe(II) ion is –100 cm^{-1} and the calculated magnetic susceptibility is shown in Figure 1.5.

Such a calculation and the comparison with the experimental magnetic susceptibility enable us to elucidate spin-orbit coupling constant, superexchange interaction constant, zero-field splitting parameters, etc.

Since this type of approach is very useful to estimate magnetic susceptibility and magnetic anisotropy of a compound, a lot of studies about magnetic cluster molecules are reported. However, this type of approach is unable to describe magnetic phase transition behavior like molecular field theory which is described in the previous section. In 1.3 and 1.4, I have introduced basic theory for magnetic analysis of molecule based magnets. In the following section, from the view point of materials chemistry and functionalites, I will introduce molecule based magnets, especially, cyano-bridged metal assemblies.

1.4 Cyano-bridged metal assemblies and their functionalities

Cyano-bridged metal assemblies are a kind of metal complex where metal ions are bridged by cyano group (M-CN-M'). Among cyano-bridged metal assemblies, one of the well-known compound is Prussian blue, $Fe^{III}_4[Fe^{II}(CN)_6]_3 \cdot 7.5H_2O$, which has three-dimensional (3D) network structure in which Fe^{II} and Fe^{III} are alternatively bridged by CN ligand with -NC-Fe^{II}-CN-Fe^{III}-NC- fashion.[61] This material has been used as blue pigment for a long time. The origin of the deep blue color in Prussian blue is metal to metal charge transfer band

between Fe^{II} and Fe^{III} due to the mixed valence state of metal ions.[62] Based on this mixed valency, electrochromic properties have been extensively investigated.[63-64] In addition, magnetic phase transition of Prussian blue was realized in 1968 with the Curie temperature (T_C) of 5.6 K.[65] In this way, Prussian blue shows interesting physical properties. Furthermore, metal ions of Fe^{II} and Fe^{III} of Prussian blue can be substituted to other metal ions and such a compound is called Prussian blue analogue. Prussian blue analogues are very attractive for designing magnetic properties and are extensively investigated from 1986.[41] In Prussian blue analogues, mainly two types of formulas are familiar, one is $M_A^{II}[M_B^{III}(CN)_6]_{2/3}\cdot 5H_2O$ and the other is $AM_A^{II}[M_B^{III}(CN)_6]_3$, where M_A and M_B are transition metal ions, and A is alkali metal ion. Both types of Prussian blue analogues take a jungle-gym-type three-dimensional network structure, while the crystal structure is different. $M_A^{II}[M_B^{III}(CN)_6]_{2/3}\cdot 5H_2O$ takes *Fm*-3*m* space group and 1/3 of $[M_B^{III}(CN)_6]$ is vacant and water molecules occupy the vacancy (Figure 1.6a).[66] $AM_A^{II}[M_B^{III}(CN)_6]_3$ prefers non-centrosymmetric *F*-43*m* space group, in which there is no vacancy in the framework structure and the interstitial sites is occupied by Alkali metal ions in alternative fashion (Figure 1.6b).[67] Our laboratory have reported various functionalities such as humidity sensitive magnetism and humidity induced magnetic pole inversion,[15] photo-induced magnetic pole inversion,[9] mixed ferro-ferri magnetism,[18-19] and two compensation temperature.[68] These unique magnetic properties and functionalities are based on the following characteristics of cyano-bridged metal assemblies. First, we can consider the magnetic interaction only among nearest neighbor metal sites because the distance between two metal centers through cyanide is sufficiently long (ca. 5 Å). Second, the magnetic interaction among nearest neighbor metal sites is strong enough to observe magnetic phase transition. Third, Prussian blue analogues can show various colors and mixed valence properties as well as original Prussian blue. These three characteristics are important to demonstrate designed magnetic properties using molecular field theory and photo-induced magnetization. Recently, in addition to $[M(CN)_6]$-based magnets, various types of cyanometalate-based complexes are utilized for molecule-based manget, e.g., heptacyanometalates ($[M(CN)_7]$) and octacyanometalates ($[M(CN)_8]$). Among them, octacyanometalates are widely investigated for molecule-based magnet and I will describe the characteristics and functionalities of octacyanometalate-based magnets.

1.5 Octacyanometalate-based magnets

Octacyanometalate ($[M(CN)_8]^{n-}$)-based magnets are expected to show various functionalities because octacyanmetalate-based magnets can take various crystal structures. Among octacyanometalate, octacyanomolybdate, octacyanotungstate, and octcyaniobate $[M(CN)_8]^{n-}$(M = Mo,W, Nb), are mainly used as building blocks of molecular magnets for the

following reasons. First, $[Mo(CN)_8]^{3-}$, $[W(CN)_8]^{3-}$, and $[Nb(CN)_8]^{4-}$ have unpaired electron, which enables the magnetic phase transition in cyano-bridged metal assemblies. Second, diffuse 4d or 5d ortibals enhance the superexchange interaction between metal centers bridged by cyanide. Third, $[Mo(CN)_8]^{n-}$ and $[W(CN)_8]^{n-}$ ions can take multiple valence states like $[Mo(CN)_8]^{3-}$/$[Mo(CN)_8]^{4-}$ and $[W(CN)_8]^{3-}$/$[W(CN)_8]^{4-}$.[69-70] Fourth, $[M(CN)_8]^{n-}$ can take various coordination geometries such as square antiprism, dodecahedron, and bicapped trigonal prism (Figure 1.7). These properties are promising for functional magnet and high T_C magnet. In fact, our laboratory have reported a zero-dimensional cluster complex with a large spin quantum number of S = 39/2,[71] a one-dimensional porous chain complex having chirality,[72] a two-dimensional layered complex which shows cooling rate dependent magnetism,[73] nanoporous three-dimensional network complex,[74] and so on (Figure 1.8-1.11). Magnetic properties of these compounds reflect their dimensionalities. Moreover, various functional molecule-based magnets have been reported in our laboratory such as photo-reversible magnetization,[75] and alcohol vapor sensitive magnet.[74] In addition, we have recently realized a vanadium-octacyanoniobate magnet which shows a high Curie temperature of 210 K,[76] magnetization-induced second harmonic generation (MSHG) in $[Mn^{II}(H_2O)_2][Mn^{II}(pyrazine)(H_2O)_2][Nb^{IV}(CN)_8]\cdot 4H_2O$,[77] humidity-induced magnetism in $Co_2[Nb(CN)_8]\cdot 8H_2O$.[78] These studies have shown that $[M(CN)_8]^{4-}$ is useful for constructing functionalized molecule based magnet.

1.6 Photo-induced magnetization in cyano-bridged metal assemblies

Photo-induced magnetization is one of the most attractive functionalities in molecule based magnet because the control of magnetization by optical stimuli can be applied to magneto-optical device. As photo-induced magnetization of hexacyanometalate-based assembly, $K_{0.2}Co_{1.4}[Fe(CN)_6]$ was reported,[46] our laboratory have reported photo-induced demagnetization and magnetic pole inversion in $Fe[Cr(CN)_6]_{2/3}\cdot 5H_2O$ and $Fe_{0.40}Mn_{0.60}[Cr(CN)_6]_{2/3}\cdot 5H_2O$,[9,79] respectively. In addition, our laboratory have reported most photo-magnetic compounds such as $Rb_{0.88}Mn[Fe(CN)_6]_{0.96}\cdot 0.5H_2O$, [12] $Cu_2[Mo(CN)_8]\cdot 8H_2O$, [11] $CsCo[W(CN)_8](3\text{-cyanopyridine})_2\cdot H_2O$,[10] $Co_3[W(CN)_8]_2(pyrimidine)_4\cdot 6H_2O$, [75] and so on. Photo-induced magnetization of these systems (other than $Fe[Cr(CN)_6]_{2/3}\cdot 5H_2O$ and $Fe_{0.40}Mn_{0.60}[Cr(CN)_6]_{2/3}\cdot 5H_2O$) is triggered by charge transfer phenomenon between metal ions, and the mechanisms of photo magnetization are mainly classified as charge transfer, charge transfer induced spin transition (CTIST), and charge transfer induced Jahn-Teller distortion as shown below.

1. Charge transfer

The photo-induced charge transfer phenomenon causes the change of electronic state of metal ions, which triggers photo-induced change of magnetization in three-dimensional

cyano-bridged metal assembly. For example, $Cu_2[Mo(CN)_8]\cdot 8H_2O$ before irradiation possesses the valence state of Cu^{II}(S = 1/2) and Mo^{IV}(S = 0), so the formula is expressed as $Cu^{II}_2[Mo^{IV}(CN)_8]\cdot 8H_2O$. After irradiating, charge transfer between Cu^{II}(S = 1/2) and Mo^{IV}(S = 0) occurs and the valence state changes to Cu^{I}(S = 0) and Mo^{V}(S = 1/2). By the irradiation of 473-nm light which correspond to the metal-to-metal charge transfer band between Cu^{II} and Mo^{IV}, the charge transfer from Mo^{IV} to Cu^{II} occurs and the electronic formula after irradiation is expressed as $Cu^{I}Cu^{II}[Mo^{V}(CN)_8]\cdot 8H_2O$. As a result, a spontaneous magnetization is generated by the magnetic interaction between the photo-produced Mo^{V}(S = 1/2) and the remaining Cu^{II}(S = 1/2). The photo-induced magnetization of this type of mechanism is caused by the mixed valence state. In class II mixed valence compound, the energy barrier appears between the orginal state and the charge separated state (Figure 1.12).[80-81] This energy barrier enables the trapping of photo-induced state, resulting in the photo-induced magnetization (Figure 1.13).

2. Charge transfer induced spin transition (CTIST)

Some photomagnetic materials show photo-induced charge transfer phenomenon and the subsequent spin transition phenomenon [charge transfer induced spin transition (CTIST)]. $CsCo[W(CN)_8](3\text{-cyanopyridine})_2\cdot 6H_2O$ is one of a typical example of this type of photomagnet. The valence state of Co and W before irradiation is Co^{III}(low-spin (LS), S = 0) and W^{IV}(S = 0), respectively. By irradiation, charge transfer from W^{IV}(S = 0) to Co^{III}(LS, S = 0) occurs and the valence state changes to Co^{II}(LS, S = 1/2) and W^{V}(S = 1/2). In this system, Co^{II} takes high-spin (HS) state rather than LS state, so spin transition takes place from Co^{II}(LS, S = 1/2) to Co^{II}(HS, S = 3/2). Magnetic interaction between Co^{II}(HS, S = 3/2) and W^{V}(S = 1/2) generates a spontaneous magnetization. In addition to $CsCo[W(CN)_8](3\text{-cyanopyridine})_2\cdot H_2O$, CTIST is also observed in $Co_3[W(CN)_8]_2(pyrimidine)_4\cdot 6H_2O$ and $K_{0.2}Co_{1.4}[Fe(CN)_6]$. The origin of the bistability derives from mixed valency, and the energy of valence isomer is more stabilized by spin transition phenomenon (Figure 1.14).

3. Charge transfer induced Jahn-Teller distortion

$Rb_{0.88}Mn[Fe(CN)_6]_{0.96}\cdot 0.5H_2O$ is representative for charge transfer induced Jahn-Teller distortion. The valence state of Mn and Fe before irradiation is Mn^{III}(HS, S = 2) and Fe^{II}(LS, S = 0). By irradiation, charge transfer between Mn^{III}(HS, S = 2) and Fe^{II}(LS, S = 0) occurs and the valence state changes to Mn^{II}(HS, S = 5/2) and Fe^{III}(LS, S = 1/2). In this system, crystal structure changes between tetragonal to cubic because of the Jahn-Teller distortion of $Mn^{III}(d^4)$ ion. In this mechanism, the mixed valency plays a main role for the bistability.

Recently, photo-induced magnetization is also reported in photo-isomerization systems using spiro-piran (SP) in $(SP)MnCr(oxalate)_3\cdot H_2O$[82] and $(SP)Fe[Fe(dithiooxalate)_3]$.[83] Still, a drastic change between paramagnetism and ferromagnetism or between antiferromagnetism and ferromagnetism was reported mostly from our laboratory in cyano-bridged metal assemblies.

1.7 Spin-crossover phenomenon

Spin-crossover is a phenomenon in which electronic state changes between high spin (HS) state and low spin (LS) state by external stimuli such as temperature, pressure and light [84-88]. Spin-crossover phenomenon in octahedral metal complex can occur in d^4 to d^7 metal ions, e.g., Cr^{II} (d^4), Mn^{III} (d^4), Mn^{II} (d^5), Fe^{III} (d^5), Fe^{II} (d^6), Co^{III} (d^6), Co^{II} (d^7).[84-95] In particular, d^6 metal ions show spin-crossover phenomenon between paramagnetic high spin state (S = 2) and diamagnetic low spin state (S = 0) (Figure 1.15), which is fascinating from the view point of application to molecular memory devices or sensors.[96-100] Before the term "Spin-crossover phenomenon" become widely used in the field of chemistry, the anomalous magnetic behavior of iron(III) complexes were reported by Cambi et al. in $[Fe^{III}(dithiocarbamate)_3]$ complex in 1931.[96] About Thirty years after this report, the first iron(II) spin-crossover complex, $[Fe(phen)_2(NCS)_2]$ (phen = 1,l0-phenanthroline) was discovered.[97] Afterwards, a lot of spin-crossover complexes have been realized and extensive studies have been executed. Spin-crossover phenomenon alters the physical properties such as color (obtical absorption properties), crystal structure, and other spectroscopic properties. Spin-crossover properties can be controlled by various chemical modifications or physical stimuli, such as substitution of spin-crossover site to a diamagnetic ion (so called metal dilution),[101] change or desorption of solvent molecule,[102] or pressure addition[103]. Furthermore, light-induced conversion from LS state to HS state was discovered and this phenomenon is called light-induced excited spin state trapping (LIESST) phenomenon.[104] Recently, the coupling effect of dielectric property and spin-crossover,[102] and host-guest chemisty of a spin-crossover compound[103] were reported. In this way, many extensive researches are executed about spin-crossover phenomenon.

1.8 Light-induced excited spin state trapping (LIESST)

In 1984, Decurtins et al. have reported a conversion from LS state to HS state by light irradiation in a spin-crossover complex of $[Fe^{II}(ptz)_6](BF_4)_2$ (ptz = 1-propyl-tetrazole).[104] This phenomenon is called Light-Induced Excited Spin State Trapping (LIESST) phenomenon, and is observed in some spin-crossover complexes.[104-107] Especially, as described in the previous section, in a Fe^{II} spin-crossover system, it is possible to change between diamagnetic LS state (S = 0) and paramagnetic HS state (S = 2). Furthermore, photo-generated HS state can be altered to the original LS state by light (reverse-LIESST phenomenon)[108], so Fe^{II} spin-crossover compounds are paid attention as a photo-reversible switching device. In multinuclear Fe^{II} spin-crossover complex, ferromagnetic or antiferromagnetic interaction by LIESST phenomenon has been reported.[109-110] However, because the reported multinuclear compounds with bulky organic ligand do not have 3-dimensional network, long range magnetic ordering cannot be generated even if it is possible to observe inner molecular short range magnetic

interaction. The LIESST phenomenon of 3-dimensional network spin-crossover compound based on $[M(CN)_4]^{n-}$ ($M=Ni^{II}$, Pd^{II}, Pt^{II}) or $[M(CN)_2]^{n-}$ ($M = Ag^{I}$,Au^{I}) have also been reported,[111-113] but the long range magnetic ordering was not observed since the central metal ions of these cyanometalates are diamagnetic and the coordination number is low. In contrast, our laboratory has reported cyano-bridged metal assemblies of $CsFe[Cr(CN)_6]\cdot 1.3H_2O$[114] and $Fe_2[Nb(CN)_8]\cdot$(3-pyridylmethanol)$_8\cdot 4.6H_2O$[115] which exhibit both spin-crossover and ferromagnetic phase transition. The coexistence of spin-crossover and ferromagnetism was observed in only these two systems and such a physical property is characteristic for a spin-crossover compound with strong magnetic interaction. In such systems, we can expect a photo-induced bulk magnetization by LIESST phenomenon, while these two compounds do not show LIESST phenomenon. To observe light-induced spin-crossover bulk magnetization, a different compound is needed.

1.9 Photo-induced spin-crossover magnetism in $Fe_2[Nb(CN)_8]$(4-pyridinealdoxime)$_8\cdot 2H_2O$

As described in previous section, spin-crossover compounds can exhibit switching of color, electric, and magnetic properties by various external stimuli, such as temperature, pressure, and light. Especially, the photo-induced phase transition from low-spin (LS) to high-spin (HS) states, which is recognized as the light-induced excited-spin-state trapping (LIESST) effect, attracts many researchers because of the possible application to molecular device. When light-induced HS sites are magnetically ordered in an infinite three-dimensional network, bulk magnetization should be observed. However, such a bulk magnetization due to light-induced spin-crossover had not been reported because the reported compounds were usually based on isolated molecular compounds or network compounds in which diamagnetic species are included between spin-crossover sites. Our laboratory has succeeded in incorporating spin-crossover sites in a three-dimensional spin-crossover system using octacyanoniobate-based cyano-bridged assembly and observed light-induced spin-crossover magnetism in $Fe_2[Nb(CN)_8]$(4-pyridinealdoxime)$_8\cdot 2H_2O$ for the first time.[127] This compound exhibits a spin-crossover phenomenon around 130 K which has Fe–NC–Nb three-dimensional cyano-bridged bimetallic framework with tetragonal $I4_1/a$ space group. At low temperature, the sample shows paramagnetism, while the irradiation of 473-nm light generates a large spontaneous magnetization with a Curie temperature (T_C) of 20 K and a coercive field (H_c) of 240 Oe at 2 K. The occurrence of photomagnetism can be explained by the following scheme. Before irradiation, paramagnetic Nb^{IV} and diamagnetic $Fe^{II}{}_{LS}$ of the low-*T* phase are connected by a CN ligand in an alternating fashion, resulting in showing paramagnetism. Irradiation with 473-nm light causes the light-induced excited-spin-state trapping (LIESST) effect on the Fe^{II} site and the magnetic spins on the photo-induced $Fe^{II}{}_{HS}$ ($S = 2$) and neighboring Nb^{IV} ($S = 1/2$)

interacts antiferromagnetically by a strong superexchange interaction through the CN ligand, resulting in bulk magnetization. Light-induced spin-crossover magnetism is important as novel type of photomagnet, so the detailed study about the crystal structure is one of an important subject for advanced research. In chapter 2, I will introduce photo-induced spin-crossover magnetism in $Fe_2[Nb(CN)_8](4\text{-pyridinealdoxime})_8 \cdot 2H_2O$ in more detail as background work, and then report the results of the room temperature single crystal X-ray diffraction measurement.

1.10 Ionic conductivity

Ionic conductivity is a measure of ability to generate current by the movement of ions.[116-119] In particular, solid substances with high ionic conductivity larger than 10^{-4} S cm^{-1} are called super-ionic conductors.[117] One of the most famous examples of super-ionic conductor is α-silver iodide (α-AgI) (Figure 1.16),[120] which is called as the first example of super-ionic conductor. α-AgI shows super-ionic conductivity of 1.9 S cm^{-1} at 473 K due to the movement of Ag^+ ions. The crystal structure shown in Figure 1.14 indicates that Ag^+ ions are disordered to many sites. Among ionic conductors, when proton is the career for ionic conductivity, the material is called proton conductor. The most famous example for proton conductor is the polymer called nafion® (Figure 1.17), which is utilized as the electrolyte layer of fuel cells. Nafion® is composed of sulfonated tetrafluoroethylene-based polymer and shows proton conductivity of 5.0×10^{-2} S cm^{-1} at room temperature due to the amount of sulfo-groups. Recently, ionic conductive coordination polymers are drawn attention[121-126]. In our laboratory, we observed super-ionic conductivity, and the interference between ionic conductivity and magnetic ordering in Prussian blue analogues, [126] and we named this phenomenon "spin-ionic". In my doctor work, the objective is to obtain new ionic conductive magnet using octacyanometalate-based magnet.

1.11 Objective

In this study, I paid attention to $[M(CN)_8]$-based magnets to demonstrate novel functionalities. I paid attention to the combination of spin-crossover phenomenon and magnetic phase transition in Fe^{II}-$[Nb(CN)_8]$ based bimetallic assemblies. In addition, to achieve ionic conductive magnetic material, I have synthesized Mn^{II}-$[Nb(CN)_8]$ based bimetallic assemblies with organic ligand. As a result, I succeeded in the demonstration of (i) light-induced spin-crossover magnetsim (Chapter 2),[127] (ii) two-step spin-crossover light-induced spin-crossover magnet (Chapter 3), and super-ionic conductive magnetism (Chapter 4).[128]

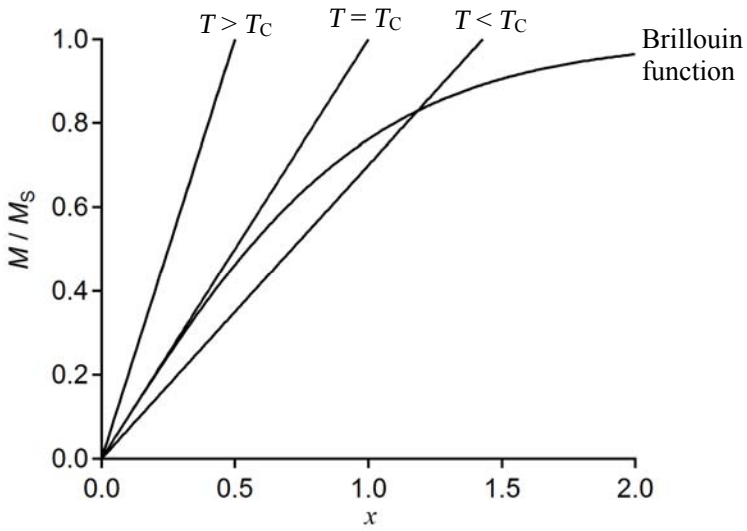

Figure 1.1 The Brillouin function and straight line at $T > T_C$, $T = T_C$, and $T < T_C$ obtained from molecular field theory. The crosspoint of two curves gives the magnetization value. Below T_C, the two curves cross at non-zero magnetization value, indicating the appearance of bulk magnetization.

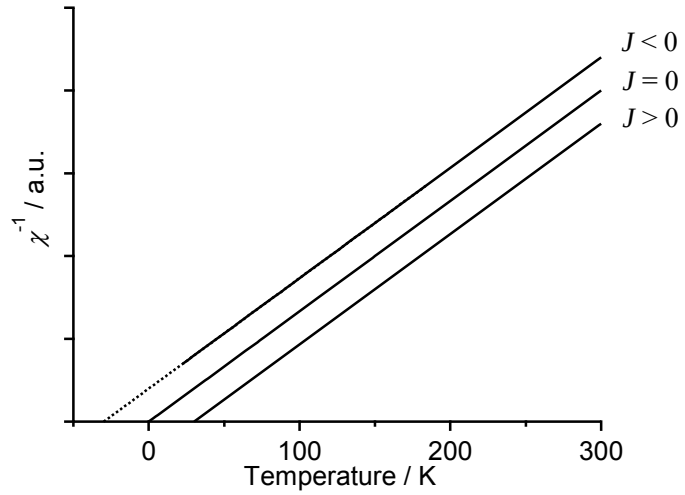

Figure 1.2 The χ^{-1} vs temperature curve obtained by Curie-Weiss law. The *x* intercept is called Weiss temperature and is negative for antiferromagnetic interaction ($J < 0$) and positive for ferromagnetic interaction ($J > 0$).

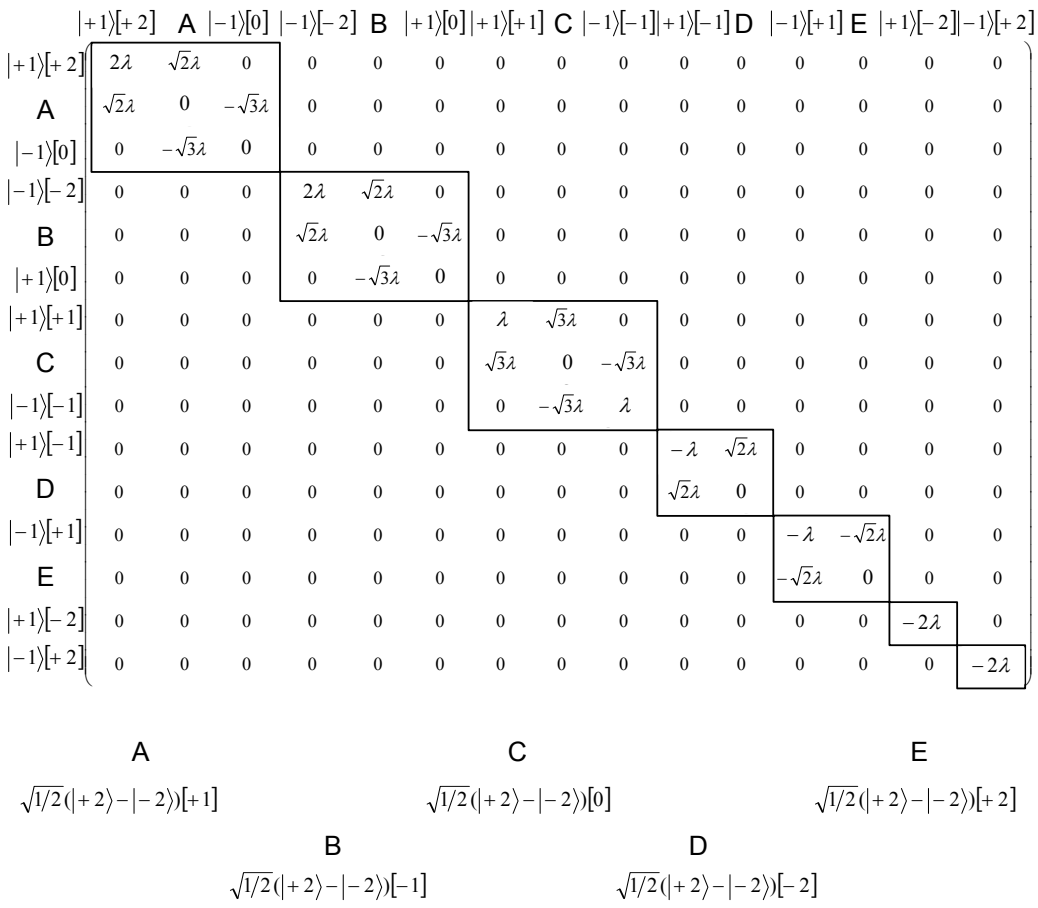

Figure 1.3 The 15 × 15 matrix obtained by considering the spin-orbit coupling between the wavefunctions of octahedral Fe^{II} ion (d^6) with $^5T_2$ term with the Hamiltonian $H = \lambda LS$. By diagonalizing this matrix, the eigenenergies and eigenfunctions are obtained.

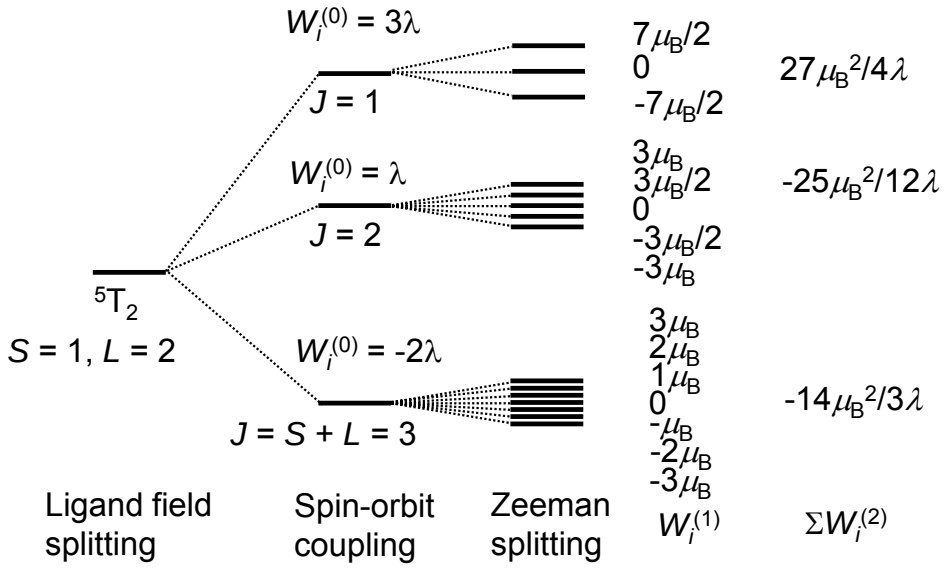

Figure 1.4 The energy separation of octahedral Fe^{II} ion (d^6) with $^5T_2$ term due to spin-orbit coupling and Zeeman splitting. The first and second order Zeeman energies ($W^{(1)}$ and $W^{(2)}$) are described in the right side.

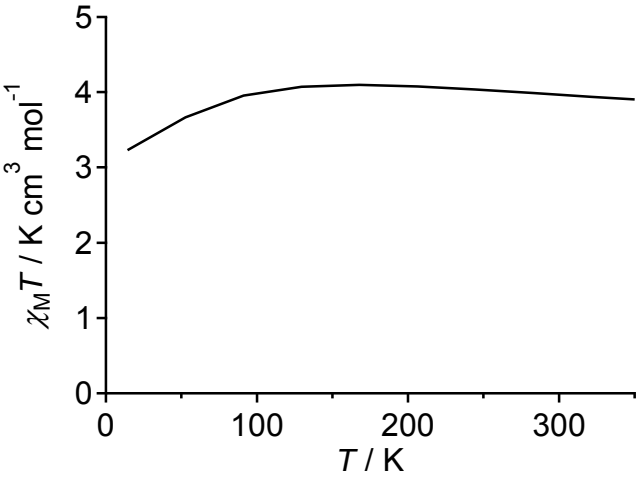

Figure 1.5 Temperature dependence of magnetic susceptibility of octahedral Fe^{II} ion (d^6) with $^5T_2$ term when λ = -100 cm^{-1}.

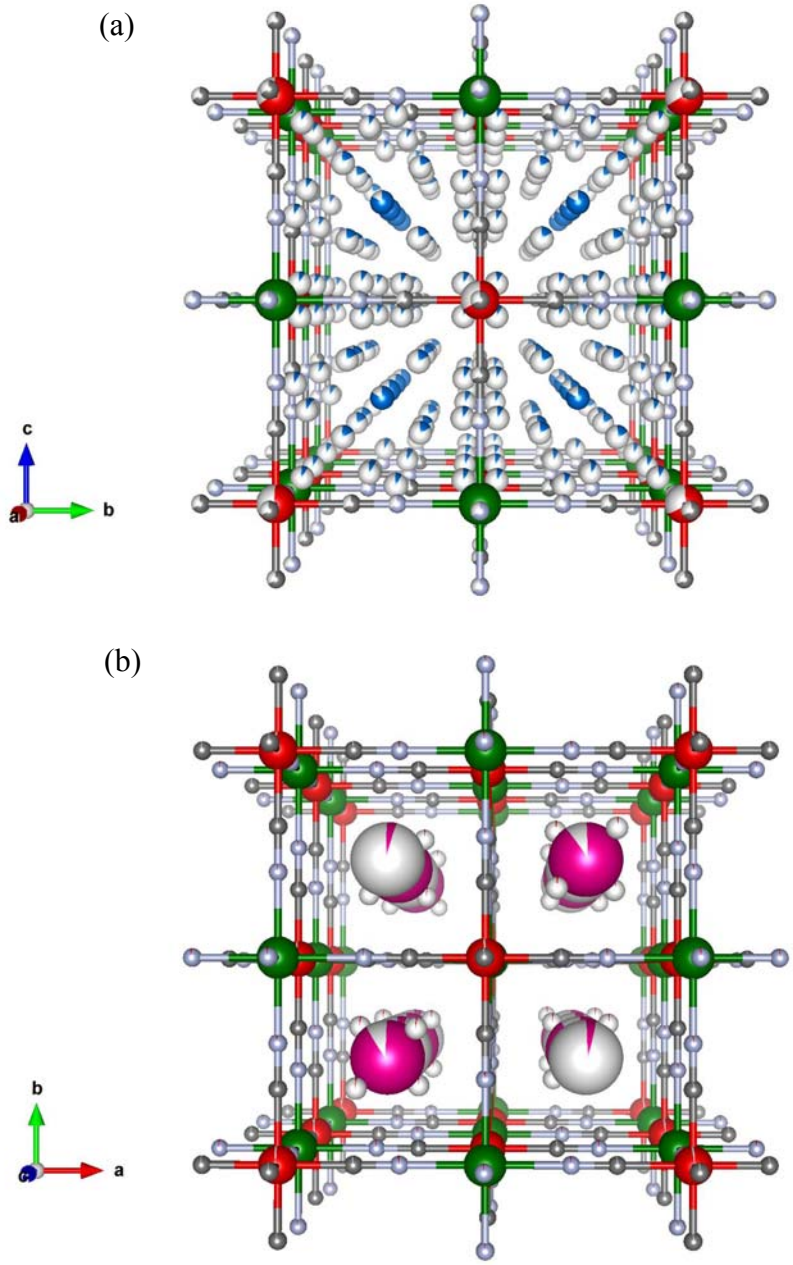

Figure 1.6 The crystal structure of Prussian blue analogues. (a) $M_A^{II}[M_B^{III}(CN)_6]_{2/3}\cdot 5H_2O$ with vacancies and water molecules. The atomic coordinates are based on reference 66. (b) $AM_A^{II}[M_B^{III}(CN)_6]_3$ with non-centrosymmetric crystal structure. The atomic coordinates are based on reference 67.

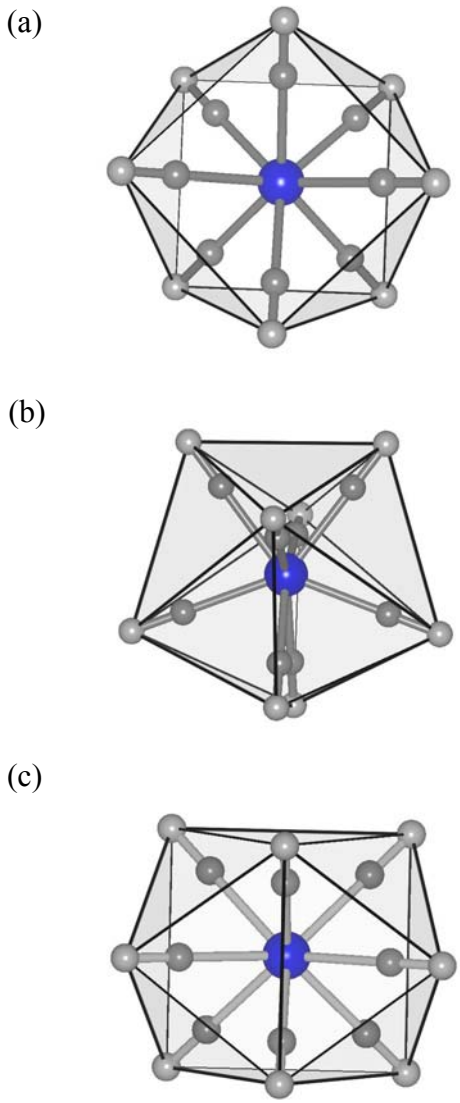

Figure 1.7 The coordination geometries of octacyanometalate. (a) Square-antiprism, (b) dodecahedron, and (c) bicapped trigonal prism.

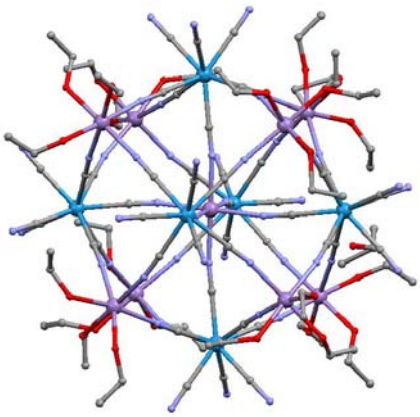

Figure 1.8 The crystal structure of octacyanometalate-based magnets of Pentadecaanuclear Mn_9W_6 cluster (0-dimensional (0-D) compound). The atomic coordinates are based on reference 71.

Reprinted with permission from Z. J. Zhong, H. Seino, Y. Mizobe, M. Hidai, A. Fujishima, S. Ohkoshi, K. Hashimoto, ***J. Am. Chem. Soc.***, 122, 2952–2953 (2000). Copyright 2000, American Chemical Society.

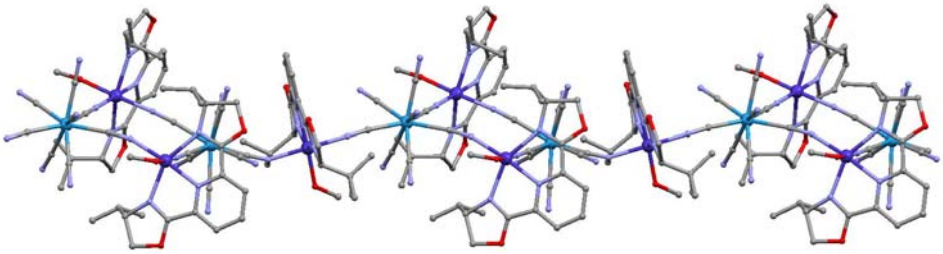

Figure 1.9 The crystal structure of octacyanometalate-based magnets of 1-D Co-W-based chain. The atomic coordinates are based on reference 72.

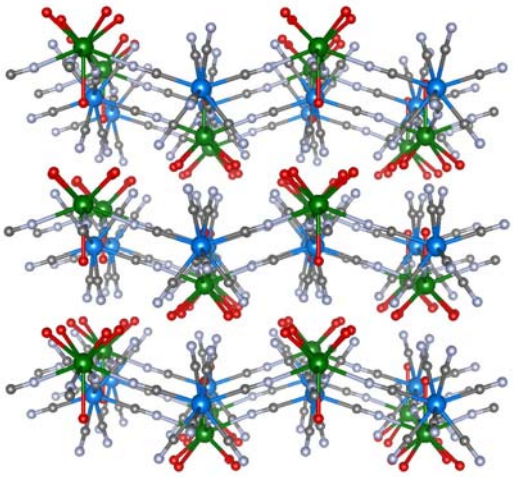

Figure 1.10 The crystal structure of octacyanometalate-based magnets of 2-D Sm-W-based magnet. The atomic coordinates are based on reference 73.

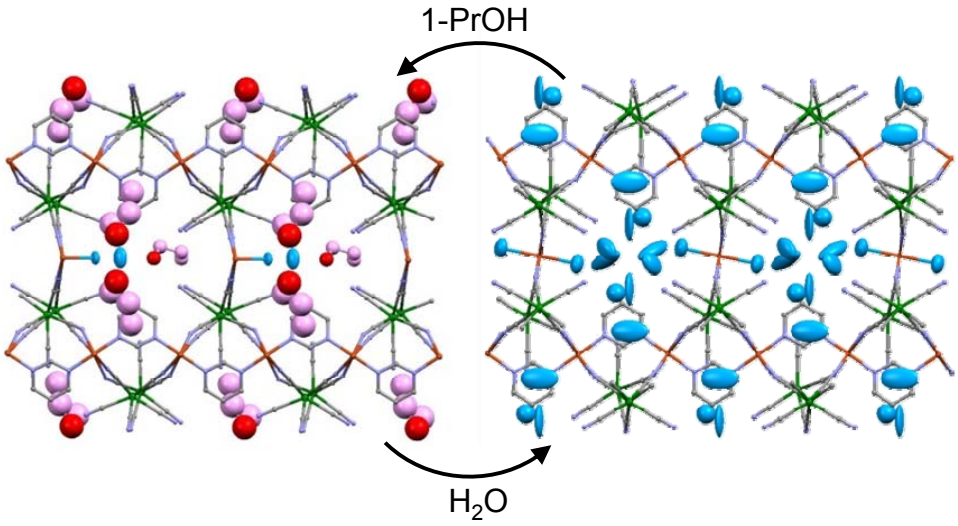

Figure 1.11 The crystal structure of octacyanometalate-based magnets of 3-D Cu-W-based magnet which shows alcohol vapor sensitivity. The crystal structure after exposure to 1-PrOH is shown in the left, and the crystal structure after exposure to water vapor is shown in the right. The atomic coordinates are based on reference 74.

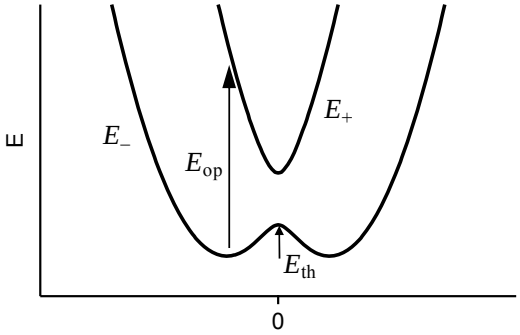

Figure 1.12 Antisymmetrical breathing nuclear coordinate Q in a mixed-valence dinuclear compound $A^{\cdot}$-B ↔ A-$B^{\cdot}$ with chemically equivalent A and B sites.

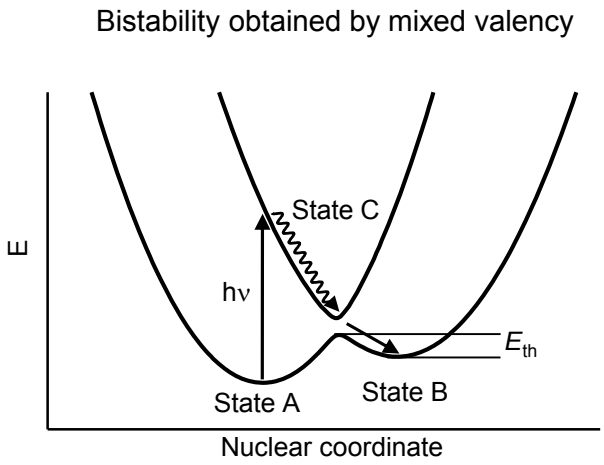

Figure 1.13 The bistability and photo-induced change of electronic state due to the energy barrier derives from the mixed valency.

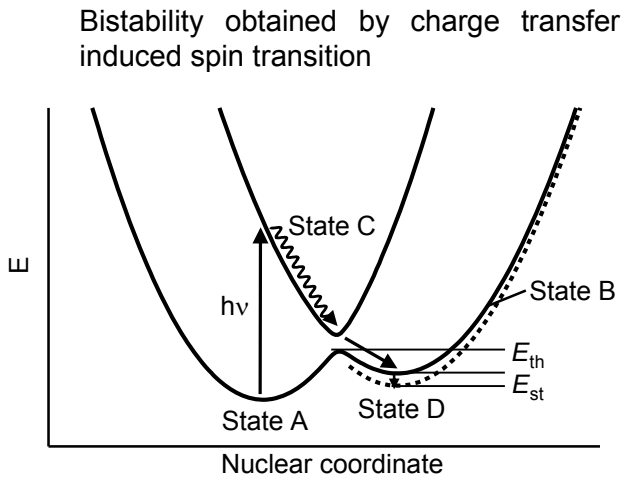

Figure 1.14 The bistability and photo-induced change of electronic state by charge transfier induced spin transition (CTIST).

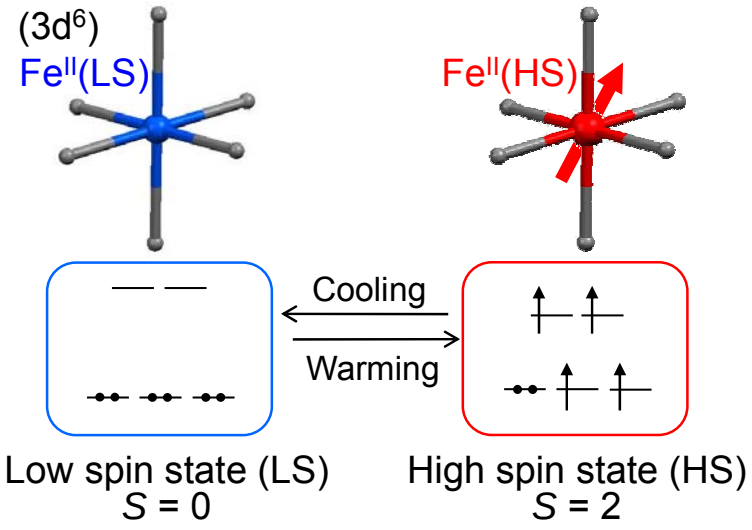

Figure 1.15 Schematic illustration of iron(II) spin-crossover phenomenon between paramagnetic high spin state ($S = 2$) and diamagnetic low spin state ($S = 0$).

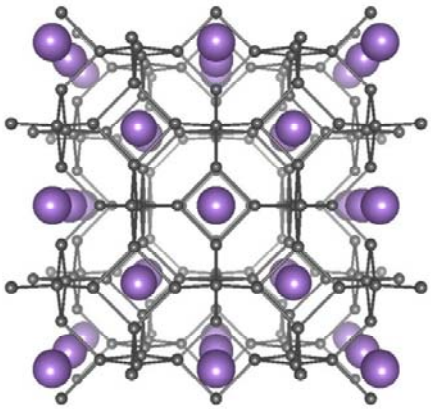

Figure 1.16 The crystal structure of α-AgI at 353 K. The atomic coordinates are based on reference 120.

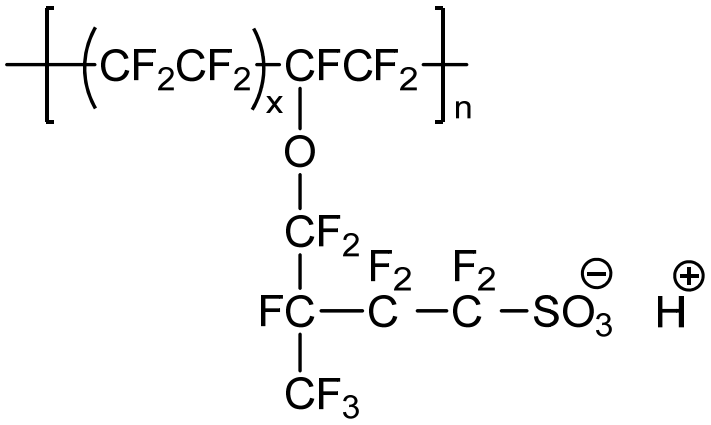

Figure 1.17 The chemical structure of the proton conductive polymer called nafion®.

Chapter 2.

本章については、5 年以内に雑誌等で刊行予定のため、非公開。

Chapter 3.

本章については、5 年以内に雑誌等で刊行予定のため、非公開。

Chapter 4.

本章については、インターネット公表に関する共著者全員の同意が得られていないため非公開。

Chapter 5.

本章については、5 年以内に雑誌等で刊行予定であるとともに、インターネット公表に関する共著者全員の同意が得られていないため、非公開。

References

[1] O. Kahn, Molecular Magnetism VCH, New York, (1993).

[2] M. Verdaguer, ***Science***, 272, 698–699 (1996).

[3] K. R. Dunbar, R. A. Heintz, ***Prog. Inorg. Chem.***, 45, 283–391 (1997).

[4] S. Ohkoshi, K. Hashimoto, ***J. Photochem. Photobiol. C***, 5, 203–223 (2004).

[5] H. Tokoro, S. Ohkoshi, ***Dalton Trans.***, 40, 6825–6833 (2011).

[6] S. Ohkoshi, H. Tokoro, ***Acc. Chem. Res.***, 45, 1749–1758 (2012).

[7] J. S. Miller, A. J. Epstein, ***Angew. Chem. Int. Ed.***, 33, 385–415 (1994).

[8] D. Gatteschi, O. Kahn, J. S. Miller, F. Palacio, Magnetic Molecular Materials Kluwer, Dordrecht, (1991).

[9] S. Ohkoshi, S. Yorozu, O. Sato, T. Iyoda, A. Fujishima, K. Hashimoto, ***Appl. Phys. Lett.***, 70, 1040–1042 (1997).

[10] Y. Arimoto, S. Ohkoshi, Z. J. Zhong, H. Seino, Y. Mizobe, K. Hashimoto, ***J. Am. Chem. Soc.***, 70, 9240–9241 (2003).

[11] S. Ohkoshi, S. Ikeda, T. Hozumi, T. Kashiwagi, K. Hashimoto, ***J. Am. Chem. Soc.***, 70, 5320–5321 (2006).

[12] S. Ohkoshi, S. Ikeda, T. Hozumi, T. Kashiwagi, K. Hashimoto, ***Chem. Mater.***, 20, 423–428 (2008).

[13] N. Ozaki, H. Tokoro, Y. Hamada, A. Namai, T. Matsuda, S. Kaneko, S. Ohkoshi, ***Adv. Funct. Mater.***, 20, 2089–2093 (2012).

[14] Y. Sato, S. Ohkoshi, K. Arai, M. Tozawa, K.Hashimoto, ***J. Am. Chem. Soc.,*** 125, 14590–14595 (2003).

[15] S. Ohkoshi, K. Arai, Y. Sato, K. Hashimoto, ***Nature Mat*erials, 3, 857–861 (2004).

[16] H. Tokoro, S. Ohkoshi, T. Matsuda, K. Hashimoto, ***Inorg. Chem.,*** 43, 5231–5236 (2004).

[17] S. Ohkoshi, T. Matsuda, H. Tokoro, K. Hashimoto, ***Chem. Mater.,*** 17, 81–84 (2005).

[18] S. Ohkoshi, T. Iyoda, A. Fujishima, K. Hashimoto, ***Phys. Rev. B***, 56, 11642–11652 (1997).

[19] S. Ohkoshi, Y. Abe, A. Fujishima, K. Hashimoto, ***Phys. Rev. Lett.***, 82, 1285–1288 (1999).

[20] S. Ohkoshi, T. Hozumi, K. Hashimoto, ***Phys. Rev. B***, 64, 132404 (2001).

[21] R. Yamada, H. Tokoro, N. Ozaki, S. Ohkoshi, ***Cryst. Growth Des.***, 12, 2013–2017 (2012).

[22] S. Ohkoshi, A. Fujishima, K. Hashimoto, ***J. Am. Chem. Soc.***, 120, 53409–5350 (1998).

[23] J. H. Van Vleck, The Theory of Electric and Magnetic susceptibilities (Oxford University Press, London, 1932).

[24] B. N. Figgis, M. A. Hitchman, Ligand Field Theory and Its Applications, WILEY-VCH, Weinheim, (1999).

[25] M. E. Lines, ***Phys. Rev.***, 131, 546–555 (1963).

[26] A. P. Ginsberg, R. L. Martin, R. W. Brookes, R. C. Sherwood, ***Inorg. Chem.***, 11, 2884–2889 (1972).

[27] C. J. O'Connor, ***Prog. Inorg. Chem.***, 29, 203–283 (1982).

[28] B. N. Figgis, J. Lewis, F. E. Mabbs, G. A. Webb, ***J. Chem. Soc. A***, 442–447 (1967).

[29] B. Bleaney, K. W. H. Stevens, ***Rep. Prog. Phys.***, 16, 108–157 (1953).

[30] J. Mulak, Z. Gajek, The Effective Crystal Field Potential (Elsevier, Amsterdam, 2000).

[31] K. S. Murray, ***Coord. Chem. Rev.***, 12, 1–35 (1974).

[32] J. C. Bonner, M. E. Fisher, ***Phys. Rev. A.***, 135, 640–658 (1974).

[33] R. Sessoli, D. Gatteschi, A. Caneschi, M. A. Novak, ***Nature***, 365, 141–143 (1993).

[34] R. Clerac, H, Miyasaka, M. Yamashita, C. Coulon, ***J. Am. Chem. Soc.***, 124, 12837–12844 (2002).

[35] R. E. P. Winpenny, ***Chem. Soc. Rev.***, 27, 447–452 (1998).

[36] G. Christou, D. Gatteschi, D. N. Hendrickson, R. Sessoli, ***MRS Bull.***, 25, 66–71 (2000).

[37] Y. Pei, M. Verdaguer, O. Kahn, ***J. Am. Chem. Soc.***, 108, 7428–7430 (1986).

[38] J. S. Miller, J. C. Calabrese, H. Rommelmann, S. R. Chittapeddi, J. H. Zhang, W. M. Reiff, A. J. Epstein, ***J. Am. Chem. Soc.***, 109, 769–781 (1987).

[39] A. Caneschi, D. Gatteschi, R. Sessoli, P. Rey, ***Acc. Chem. Res.***, 22, 392–398 (1987).

[40] M. Kinoshita, P. Turek, M. Tamura, K. Nozawa, D. Shiomi, Y. Nakazawa, M. Ishikawa, M. Takahashi, K. Awaga, T. Inabe, Y. Maruyama, ***Chem. Lett.*** 1225–1228 (1991).

[41] D. Babel, ***Comments Inorg. Chem.***, 5, 285–320 (1986).

[42] S. Ferlay, T.Mallah, R. Ouahès, P. Veillet, M. Verdaguer, ***Nature***, 378, 701–703 (1995).

[43] S. M. Holmes, G. S. Girolami, ***J. Am. Chem. Soc.***, 121, 5593–5594 (1999).

[44] Ø. Hatlevik, W. E. Buschmann, J. Zhang, J. L. Manson, J. S. Miller, ***Adv. Mater.***, 11, 914–918 (1999).

[45] S. Ohkoshi, M. Mizuno, G. J. Hung, K. Hashimoto, ***J. Phys. Chem. B***, 104, 9365–9367 (2000).

[46] O. Sato, T. Iyoda, A. Fujishima, K. Hashimoto, ***Science***, 272, 704–705 (1996).

[47] A. Bleuzen, C. Lomenech, V. Escax, F. Villain, F. Varret, C. Cartier dit Moulin, M. Verdaguer, ***J. Am. Chem. Soc.***, 122, 6648–6652 (1995).

[48] D. M. Pajerowski, M. J. Andrus, J. E. Gardner, E. S. Knowles, M. W. Meisel, D. R. Tahlam, ***J. Am. Chem. Soc.***, 132, 4058–4059 (2010).

[49] J. Larionova, R. Clerac, J. Sanchiz, O. Kahn, S. Golhen, L. Ouahab, ***J. Am. Chem. Soc.***, 120, 13088–13095 (1998).

[50] J. Milon, M. C. Daniel, A. Kaiba, P. Guionneau, S. Brandes, J.-P. Sutter, ***J. Am. Chem. Soc.***, 129, 13872-13878 (2007).

[51] K. Tomono, Y. Tsunobuchi, K. Nakabayashi, S. Ohkoshi, ***Inorg. Chem.***, 49, 1298–1300 (2010).

[52] X.-Y. Wang, A. V. Prosvirin, K. R. Dunbar, ***Angew. Chem. Int. Ed.***, 49, 5081–5084 (2010).

[53] R. Garde, C. Desplanches, A. Bleuzen, P. Veillet, M. Verdaguer, ***Mol. Cryst. Liq. Cryst.***, 334, 587–595 (1999).

[54] Z. J. Zhong, H. Seino, Y. Mizobe, M. Hidai, M. Verdaguer, S. Ohkoshi, K. Hashimoto, ***Inorg. Chem.***, 39, 5095–5101 (2000).

[55] B. Sieklucka, J. Szklarzewicz, T. J. Kemp, W. Errington, ***Inorg. Chem.***, 39, 5156–5158 (2000).

[56] R. Pradhan, C. Desplanches, P. Guionneau, J.-P. Sutter, ***Inorg. Chem.***, 42, 6607–6609 (2003).

[57] D. Pinkowicz, R. Podgajny, M. Bałanda, M. Makarewicz, B. Gaweł, W. Łasocha, B. Sieklucka, ***Inorg. Chem.***, 47, 9745–9747 (2008).

[58] J. M. Herrera, P. Franz, R. Podgajny, M. Pilkington, M. Biner, S. Decurtins, H.Stoeckli-Evans, A. Neels, R. Garde, Y. Dromzée, M. Julve, B.Sieklucka, K. Hashimoto, S. Ohkoshi, M. Verdaguer, ***C. R. Chim.***, 11, 1192–1199 (2008).

[59] R. L. Bris, Y. Tsunobuchi, C. Mathoniere, H. Tokoro, S. Ohkoshi, N. Ould-Moussa, G. Molnar, A. Bousseksou, J. F. Letard, ***Inorg. Chem.***, 51, 2852–2859 (2012).

[60] L. Néel, ***Ann. Phys.*** 3, 137–198 (1948).

[61] H. J. Buser, D. Schwarzenbach, W. Petter, A. Ludi, ***Inorg. Chem.***, 11, 2704–2710 (1977).

[62] C. Creutz, ***Prog. Inorg. Chem.***, 30, 1–47 (1983).

[63] B. Mayoh, P. Day, ***J. Chem. Soc., Dalton Trans.***, 1483–1486 (1976).

[64] K. Itaya, I. Uchida, V. D. Neff, ***Acc. Chem. Res.***, 162–168 (1986).

[65] A. Ito, M. Suenaga, K. Ono, ***J. Chem. Phys.***, 48, 3597–3599, (1968).

[66] T. Matsuda, H. Tokoro, M. Shiro, K. Hashimoto, S. Ohkoshi, ***Acta Cryst.***, E64, i11–i12, (2008).

[67] S. Ohkoshi, T. Matsuda, S. Saito, T. Nuida, H. Tokoro, ***J. Phys. Chem. C***, 112, 13095–13098 (2008).

[68] S. Ohkoshi, Y. Abe, A. Fujishima, K. Hashimoto, ***Phys. Rev. Lett.***, 82, 1285–1288 (1999).

[69] H. Hennig, A. Rehorek, D. Rehorek, P. Thomas, ***Inorg. Chim. Acta***, 86, 41–49 (1984).

[70] D. Rehorek, J. Salvetter, A. Hantschmann, H. Hennig, Z. Stasicka, A. Chodkowska, ***Inorg. Chim. Acta.***, 37, L471–L472 (1979).

[71] Z. J. Zhong, H. Seino, Y. Mizobe, M. Hidai, A. Fujishima, S. Ohkoshi, K. Hashimoto, ***J. Am. Chem. Soc.***, 122, 2952–2953 (2000).

[72] S. Chorazy, K. Nakabayashi, K. Imoto, J. Mlynarski, B. Sieklucka, S. Ohkoshi, ***J. Am. Chem. Soc.***, 134, 16151−16154 (2012).

[73] T. Hozumi, S. Ohkoshi, H. Seino, Y. Mizobe, K. Hashimoto, ***J. Phys. Chem. B***, 107, 11571−11574 (2003).

[74] S. Ohkoshi, Y. Tsunobuchi, H. Takahashi, T. Hozumi, M. Shiro, K. Hashimoto, ***J. Am. Chem. Soc.***, 129, 3084–3085 (2007).

[75] S. Ohkoshi, Y. Hamada, T. Matsuda, Y. Tsunobuchi, H. Tokoro, ***Chem. Mater.***, 20, 3048–3054 (2008).

[76] K. Imoto, M. Takemura, H. Tokoro, S. Ohkoshi, ***Eur. J. Inorg. Chem.***, 2649–2652 (2012).

[77] D. Pinkowicz, R. Podgajny, W. Nitek, M. Rams, A. M. Majcher, T. Nuida, S. Ohkoshi, B. Sieklucka, ***Chem. Mater.***, 23, 21–31 (2011).

[78] K. Imoto, D. Takahashi, Y. Tsunobuchi, M. Arai, W. Kosaka, H. Tokoro, S. Ohkoshi, ***Eur. J. Inorg. Chem.***, 4079–4082 (2010).

[79] S. Ohkoshi, Y. Einaga, A. Fujishima, K. Hashimoto, ***J. Electrochem. Soc.***, 473, 245–249 (1999).

[80] M. B. Robin, P. Day, ***Adv. Inorg. Chem. Radiochem.***, 10, 247−422 (1967).

[81] C. Creutz, H. Taube, ***J. Am. Chem. Soc.***, 91, 3988−3989 (1969).

[82] S. Benard, E. Riviere, P. Yu, K. Nakatani, J. F. Delouis, ***Chem. Mater.***, 13, 159–162 (2001).

[83] N. Kida, M. Hitaka, I. Kashima, M. Okubo, M. Itoi, M. Enomoto, K. Kato, M. Takata, N. Kojima, ***J. Am. Chem. Soc.***, 131, 212–220 (2009).

[84] P. Gutlich and H. A. Goodwin, (eds.) Spin crossover in transition metal compounds I, II, III. ***Top. Curr. Chem.***, 233–235 (2004).

[85] E. Konig, ***Prog. Inorg. Chem.***, 35, 527–622 (1987).

[86] P. Gutlich, A. Hauser, H. Spiering, ***Angew. Chem. Int. Ed.***, 33, 2024–2054 (1994).

[87] J. A. Real, E. Andres, M. C. Munos, M. Julve, T. Granier, A. Bousseksou, F. Vallet, ***Science***, 268, 265–267 (1995).

[88] O. Kahn, C. J. Martinez, ***Science***, 279, 44–48 (1998).

[89] D. M. Halepoto, D. G. L. Holt, L. F. Larkworthy, G. J. Leigh, D. C. Povey, G. W. Smith, ***J. Chem. Soc., Chem. Comm.***, 1322–1323 (1989).

[90] P. G. Sim, E. Sinn, ***J. Am. Chem. Soc.***, 241–243 (1981).

[91] P. N. Martinho, B. Gildea, M. M. Harris, T. Lemma, A. D. Naik, H. M.-Bunz, T. E. Keyes, Y. Garcia, G. G. Morgan, ***Angew. Chem. Int. Ed.***, 51, 12597–12601 (2012).

[92] D. Cozak, F. Gauvin, J. Demers, ***Can. J. Chem.***, 64, 71–75 (1986).

[93] S. Hayami, Z. Gu, H. Yoshiki, A. Fujishima, O. Sato, ***J. Am. Chem. Soc.***, 123, 11644–11650 (2001).

[94] W. Klaui, W. Eberspach, P. Gutlich, ***Inorg. Chem.***, 26, 3977–3982 (1987).

[95] S. Brooker, P. G. Plieger, B. Moubaraki, K. S. Murray, ***Angew. Chem. Int. Ed.***, 38, 408–410 (1999).

[96] L. Cambi, L. Szego, ***Ber. Dtsch Ges.*** 64, 2591–2598 (1931).

[97] W. A. Baker, H. M. Bobonich, ***Inorg. Chem.***, 3, 1184–1188 (1964).

[98] J. F. Letard, P. Guionneau, E. Codjovi, O. Lavastre, G. Bravic, D. Chasseau, O. Kahn, ***J. Am. Chem. Soc.***, 119, 10861–10862 (1997).

[99] K. Boukheddaden, I. Shteto, B. Hoo, F. Varret, ***Phys. Rev. B***, 62, 14796–14805 (2000).

[100] V. Niel, A. L. Thompson, M. C. Munoz, A. Galet, A. E. Goeta, J. A. Real, ***Angew. Chem. Int. Ed.***, 42, 3760–3763 (2003).

[101] P. Gutlich, R. Link, G. Steinhauser, ***Inorg. Chem.***, 17, 2509–2514 (1978).

[102] M. Nihei, L. Han, H. Oshio, ***J. Am. Chem. Soc.***, 129, 5312–5313 (2007).

[103] A. Bousseksou, G. Molnar, G. Matouzenko, ***Eur. J. Inorg. Chem.***, 4353–4369 (2004).

[104] S. Decurtins, P. Gutlich, C. P. Kohler, H. Spiering, A. Hauser, ***Chem. Phys. Lett.*** 105, 1–4 (1984).

[105] A. Bousseksou, G. Molnar, P. Demont, J. Menegotto, ***J. Mater. Chem.***, 13, 2069–2071 (2003).

[106] G. J. Halder, C. J. Kepert, B. Moubaraki, K. S. Murray, J. D. Cashion, ***Science***, 298, 1762–1765 (2002).

[107] M. Ohba, K. Yoneda, G, Agusti, M. C. Munoz, A. B. Gaspar, J. A. Real, M. Yamasaki, H. Ando, Y. Nakao, S. Sakaki, S. Kitagawa, ***Angew. Chem. Int. Ed.***, 48, 4767–4771 (2009).

[108] A. Hauser, ***J. Chem. Phys.***, 94, 2741–2748 (1991).

[109] N. Ould-Moussa, E. Trzop, S. Mouri, S. Zein, G. Molnar, A. B. Gaspar, E. Collet, M. Buron-Le Cointe, J. A. Real, S. Borshch, K. Tanaka, H, Cailleau, A. Bousseksou, ***Phys. Rev. B***, 75, 054101/1–8 (2007).

[110] E. Breuning, M. Ruben, J.-M. Lehn, F. Renz, Y. Garcia, V. Ksenofontov, P. Gutlich, E. Wegelius, K. Rissanen, ***Angew. Chem. Int. Ed.***, 39,2504–2507 (2000).

[111] T. Kitazawa, Y. Gomi, M. Takahashi, M. Takeda, M. Enomoto, A. Miyazaki, T. Enoki, ***J. Mater. Chem.***, 6, 119–121 (1996).

[112] V. Niel, J. M. Agudo-Martinez, M. C. Munoz, A. B. Gaspar, J. A. Real, ***Inorg. Chem.***, 40, 3838–3839 (2001).

[113] P. D. Southon, L. Liu, E. A. Fellows, D. J. Price, G. J. Halder, K. W. chapman, B. Moubaraki, K. S. Murray, J. F. Letard, C. J. Kepert, ***J. Am. Chem. Soc.***, 131,

10998–11009 (2009).

[114] W. Kosaka, K. Nomura, K. Hashimoto, S. Ohkoshi, ***J. Am. Chem. Soc.***, 127, 8590–8591 (2005).

[115] M. Arai, W. Kosaka, T. Matsuda, S. Ohkoshi, ***Angew. Chem. Int. Ed.*** 47, 6885–6887 (2008)

[116] P.Colomban, ***J. Mol. Struct.***, 177, 277–308 (1988).

[117] P. Colomban, *Proton conductors*; Cambridge University Press: U.K., 1992.

[118] B. C. Steele, A. Heinzel, ***Nature***, 414, 345–352 (2001).

[119] K. D. Kreuer, S. J. Paddison, E. Spohr, M. Schuster, ***Chem. Rev.***, 104, 4637–4678 (2004).

[120] M. Suzuki and H. Okazaki, ***Phys. Stat. Sol. A***, 42, 831–836 (1977).

[121] M. Sadakiyo, H. Ōkawa, A. Shigematsu, M. Ohba, T. Yamada, H. Kitagawa, ***J. Am. Chem. Soc.***, 134, 5472–5475 (2012).

[122] H. Ōkawa, A. Shigematsu, M. Sadakiyo, T. Miyagawa, K. Yoneda, M. Ohba, H. Kitagawa, ***J. Am. Chem. Soc.***, 131, 13516–13517 (2009).

[123] E. Pardo, C. Train, G. Gontard, K. Boubekeur, O. Fabelo, H. Liu, B. Dkhil, F. Lloret, K. Nakagawa, H. Tokoro, S. Ohkoshi, M. Verdaguer, ***J. Am. Chem. Soc.***, 133, 15328−15331 (2011).

[124] S. Bureekaew, S. Horike, M. Higuchi, M. Mizuno, T. Kawamura, D. Tanaka, N. Yanai, S. Kitagawa, ***Nature Mater.***, 8, 831–836 (2009).

[125] J. A. Hurd, R. Vaidhyanathan, V. Thangadurai, C. I. Ratcliffe, I. L. Moudrakovski, G. K. H. Shimizu, ***Nature Chem.***, 1, 705–710 (2009).

[126] S. Ohkoshi, K. Nakagawa, K. Tomono, K. Imoto, Y. Tsunobuchi, H. Tokoro, ***J. Am. Chem. Soc.***, 132, 6620–6621 (2010).

[127] S. Ohkoshi, K. Imoto, Y. Tsunobuchi, S. Takano, H. Tokoro, ***Nature Chemistry***, 3, 564–569 (2011).

[128] K. Imoto, K. Nakagawa, H. Miyahara, S. Ohkoshi, ***Cryst. Growth Des.***, 13, 4673–4677 (2013).

[129] G. M. Sheldrick, ***Acta Crystallogr.*** A64, 112–122 (2008).

[130] A. P. Ginsberg and M. E. Lines, ***Inorg. Chem.***, 11, 2289–2290 (1972).

List of papers related to the thesis

(1) “Light-induced spin-crossover magnet”
S. Ohkoshi, K. Imoto, Y. Tsunobuchi, S. Takano, and H.Tokoro,
Nature Chemistry, 3, 564-569 (2011).

This paper corresponds to Chapter 2.

(2) “Super-Ionic Conductive Magnet Based on a Cyano-Bridged Mn-Nb Bimetal Assembly”
K. Imoto, K. Nakagawa, H. Miyahara, and S. Ohkoshi,
Cryst. Growth Des., 13, 4673-4677 (2013).

This paper corresponds to Chapter 4.

Acknowledgement

First of all, I would like to express my great gratitude to my supervisor, Prof. Shin-ichi Ohkoshi. He has guided me into this interesting research field. His belief in science, enthusiasm for experiments, and logical thinking gave me a deep impression. I really appreciate him in all aspects of my research.

I would like to thank Dr. Hiroko Tokoro for teaching me a lot of experimental techniques. Her attitude and carefulness for experiments taught me about many important things for experiment. I acknowledge Dr. Koji Nakabayashi, Dr. Kosuke Nakagawa, and Ms. Asuka Namai for a lot of useful advice and discussions.

I am grateful to Dr. Kimiko Saeki and Dr. Aiko Kamitsubo for the elemental analysis of organic elements and Dr. Shigeru Otsuka for the measurement of SEM images.

I am also greatly indebted to all the members of Ohkoshi laboratory, Mr. Fumiyoshi Hakoe, Mr. Noriaki Ozaki, Ms. Marie Yoshikiyo, Mr. Yoshikazu Umeta, Ms. Miho Takemura, Mr. Yasuto Miyamoto, Mr. Tomomichi Nasu, Mr. Kenji Tanaka, Mr. Hiroyuki Miyahara, Mr. Takashi Fujimoto, Mr. Masaya Komine, Mr. Tomoya Ogino, Mr. Kohei Okamoto, and all ex-lab members for their help and cooperation.

Finally, I would like to thank my father, mother, and brother for their understanding, support, and encouragement throughout my study.

Kenta Imoto